JAERI-Research
98-049

DESIGN OF ITER NEUTRON MONITOR USING MICRO FISSION CHAMBERS

August 1998

Takeo NISHITANI, Larry C. JOHNSON*, Katsuyuki EBISAWA,
Chris WALKER**, Toshiro ANDO and Satoshi KASAI

日本原子力研究所
Japan Atomic Energy Research Institute

本レポートは，日本原子力研究所が不定期に公刊している研究報告書です。
入手の問合わせは，日本原子力研究所研究情報部研究情報課（〒319-1195　茨城県那珂郡東海村）あて，お申し越しください。なお，このほかに財団法人原子力弘済会資料センター（〒319-1195　茨城県那珂郡東海村日本原子力研究所内）で複写による実費頒布をおこなっております。

This report is issued irregularly.
Inquiries about availability of the reports should be addressed to Research Information Division, Department of Intellectual Resources, Japan Atomic Energy Research Institute, Tokai-mura, Naka-gun, Ibaraki-ken, 319-1195, Japan.

編集兼発行　　日本原子力研究所

JAERI-Research 98-049

Design of ITER Neutron Monitor using Micro Fission Chambers

Takeo NISHITANI, Larry C. JOHNSON*, Katsuyuki EBISAWA+,
Chris WALKER**, Toshiro ANDO+ and Satoshi KASAI++

Department of Fusion Plasma Research
Naka Fusion Research Institute
Japan Atomic Energy Research Institute
Naka-machi, Naka-gun, Ibaraki-ken

(Received July 28, 1998)

We are designing micro fission chambers, which are pencil size gas counters with fissile material inside, to be installed in the vacuum vessel as neutron flux monitors for ITER. We found that the ^{238}U micro fission chambers are not suitable because the detection efficiency will increase up to 50% in the ITER life time by breading ^{239}Pu. We propose to install ^{235}U micro fission chambers on the front side of the back plate in the gap between adjacent blanket modules and behind the blankets at 10 poloidal locations. One chamber will be installed in the divertor cassette just under the dome. Employing both pulse counting mode and Campbelling mode in the electronics, we can accomplish the ITER requirement of 10^7 dynamic range with 1 ms temporal resolution, and eliminate the effect of gamma-rays. We demonstrate by neutron Monte Carlo calculation with three-dimensional modeling that we avoid those detection efficiency changes by installing micro fission chambers at several poloidal locations inside the vacuum vessel.

Keywords: Neutron Monitor, Micro Fission Chamber, ITER, Fusion Power, Campbelling Mode, MCNP, Neutron Source Strength

---

This work is conducted as an ITER Engineering Activities as this report coresponds to ITER Design Task Agreement on "Diagnostics Design" (S 55 TD 02 FJ).

+ Department of ITER Project
++ Department of Fusion Engineering Research
* ITER Joint Central Team, San Diego
** ITER Joint Central Team, Garching

マイクロフィッションチェンバーを用いたITER用中性子モニターの設計

日本原子力研究所那珂研究所炉心プラズマ研究部
西谷　健夫・ Larry C. JOHNSON*・海老沢克之+
Chris WALKER**・安東　俊郎+・河西　敏++

（1998年7月28日受理）

マイクロフィッションチェンバー（鉛筆サイズの核分裂計数管）を使用したITER用中性子モニターの設計を行った。マイクロフィッションチェンバーに使用する核分裂物質としては、^{238}Uは^{239}Puの増殖によりITERの寿命中、感度が５０％も増加するので、^{235}Uを採用した。このマイクロフィッションチェンバーを、遮蔽ブランケットとそのバックプレートに間、及び隣合う遮蔽ブランケットの間隙を一対として１０箇所、及びダイバータカセットのドームの下に１箇所配置した。 ITERでは中性子モニターに対し、７桁の測定レンジと1msの時間分解能が要求されているが、１つの検出器に対しパルス計数モードとキャンベルモードの回路系を併用することにより、これを実現できることを示した。また各マイクロフィッションチェンバーの出力を用いて、プラズマの位置によらず中性子発生率を測定できることを、ITERの３次元モデルを使用した中性子のモンテカルロ計算により確認した。

本研究はＩＴＥＲ工学設計活動の一環として実施したもので、本報告は設計タスク協定(S 55 TG 02 FJ)に基づくものである。

那珂研究所：〒311-0193　茨城県那珂郡那珂町向山801-1
+　　ITER 開発室
++　核融合工学部
＊　　ITER サンディエゴ共同センター
＊＊　ITER ガルヒンク共同センター

Contents

目　　次

1. INTRODUCTION

1.1 Functions

The absolute measurement of neutron source strength is very important for controlling the fusion power in a fusion experimental reactor such as ITER. In present large tokamaks such as JET[1], TFTR[2] or JT-60U[3], the neutron source strength measurement has been carried out using ^{235}U or ^{238}U fission chambers installed outside the vacuum vessel. Detection efficiencies of those detectors are easily affected by surrounding equipment such as other diagnostics or heating systems. Because ITER has a thick blanket and vacuum vessel, detectors outside the vacuum vessel may not measure the neutron source strength with sufficient accuracy. We are designing micro fission chambers, which are pencil size gas counters with fissile material inside, to be installed in the vacuum vessel as neutron flux monitors for ITER[4-6]. By installing the detectors at several poloidal angles, this neutron monitor system may reject or reduce the error of the neutron source strength measurement caused by the change of the plasma position and/or shape. This report provides the conceptual feasibility study of this neutron monitor system.

The Neutron monitors have important functions in providing measurements for machine protection and plasma control, and will continue to be needed for performance evaluation and optimization, and for physics understanding. The primary function is measurement of the total neutron source strength, hence the fusion power. Table 1-1 lists the plasma parameter for with the micro fission chambers can provide measurements.

Table 1-1. System function of the neutron monitor.

Name of System	Category & Meas. #	Plasma Parameters
Micro fission chambers	(1)#7	Total neutron flux & emission profile (with 5.5.B.01, 5.5.B.02 and 5.5.B.04)

Category (1) : Measurements for machine protection and plasma control.
Measurement #7 : Total neutron flux and emission profile

1.2 Design Requirements

Table 1-2 specifies parameter ranges, temporal resolutions, and measurement accuracy. So the neutron detector has to have wide dynamic range and fast response. From the technical point of view, it should be insensitive to gammas and robust in the ITER environment of high levels of radiation, electro-magnetic noise, and

mechanical vibrations. The detection efficiency must be stable during the ITER operation life, and the system should be easily calibrated. In ITER, conventional neutron monitors installed outside the vacuum vessel and in-vessel neutron monitor using micro fission chamber are proposed for the neutron source strength measurement. These will be augumented by neutron cameras [7], which provide local and global neutron emmision rate. However, it needs the Abel inversion or tomography technique to get the neutron source profile.

Table 1-2. Requirement for neutron monitor.

Parameter	Parameter range	Spatial resolution	Time resolution	Accuracy
Neutron source strength	10^{14}-10^{21} n s^{-1}	integral	1 ms	10 %
Fusion power	≤2 GW	integral	1 ms	10 %

2. CONCEPTUAL DESIGN

2..1 Micro Fission Chamber

A micro fission chamber is a pencil size gas counter with fissile material inside, which was developed as an in-core monitor for fission reactors. Figure 2-1 shows the schematics of the typical micro fission chamber with wide dynamic range which is commercially available except sheath which is specially designed for ITER. We add the sheath for the chamber from two reasons. One is to shield electro-magnetic noise. Another is safety reason. The sheath will prevent the uranium contamination inside the vacuum vessel when the uranium is leaked from the chamber housing. In this detector, about 12 mg of UO_2 is coated on the cylindrical electrode and 14.6 atm of Ar + 5% N_2 gas is filled between the electrodes.

This type micro fission chamber can be operated in pulse counting mode at low neutron flux, in Campbelling (mean square voltage) mode at medium flux and in current mode at high flux. Combinations of those operation modes may provide wide dynamic range of 10^{10} with temporal resolution of 1 ms, which satisfies the ITER requirement. The most popular candidates for a fissile material in the micro fission chamber are ^{235}U, ^{238}U and ^{232}Th. ^{235}U has large fission cross-section for thermal neutrons, the others have fission cross-sections with a threshold of ~1 MeV as shown in Fig.2-2. The fission cross-section of ^{232}Th is several times lower than that of ^{238}U. So we discuss ^{235}U and ^{238}U as the candidate of the fissile material for the micro fission chamber.

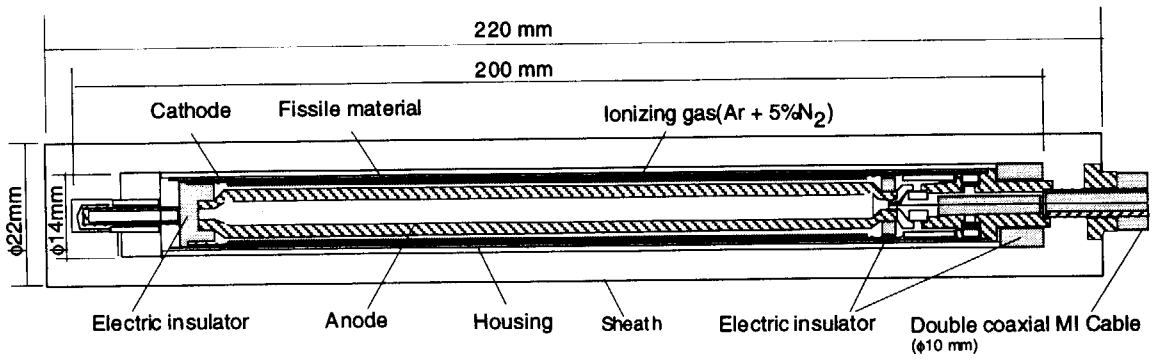

Fig. 2-1. Schematics of typical micro fission chamber. Fissile material such as ^{235}U is coated on the cylindrical electrode. Ionizing gas of Ar + 5% N_2 (14.6 atm) is filled between the electrodes. The sheath is specially designed for ITER.

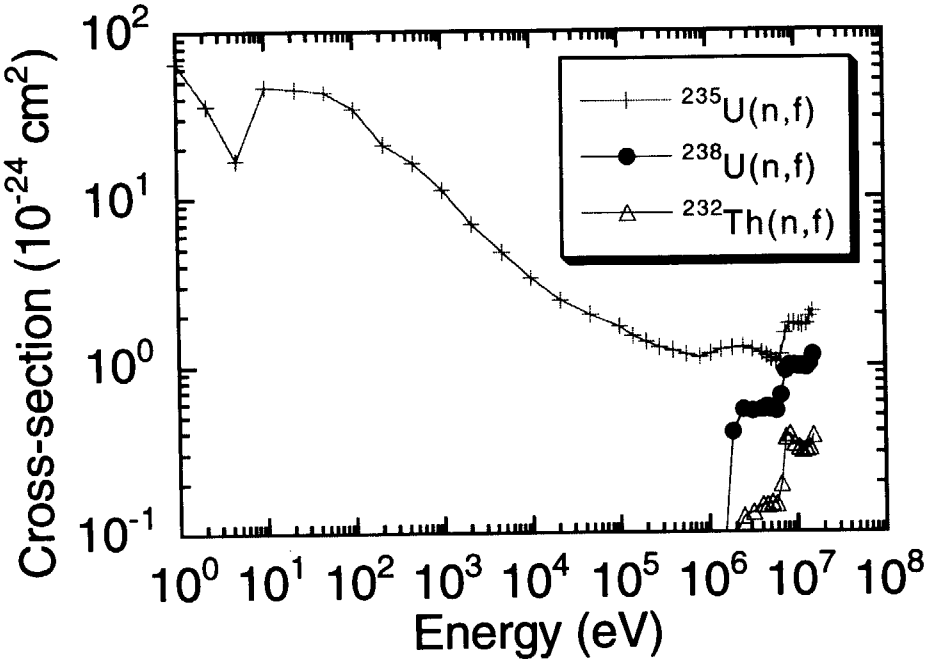

Fig. 2-2. Fission cross-section of ^{235}U, ^{238}U and ^{232}Th.

Mineral insulated (MI) cable is used to transfer signals, so that we can install micro fission chambers inside the vacuum vessel in the same manner as magnetic probes. Cooling of the detectors is necessary in order to keep the operational temperature below 300°C in the presence of strong nuclear heating inside the vacuum vessel. The typical performance of the micro fission chamber of ^{235}U with the dimension shown in Fig.2-1 is listed in Table 2-1.

Table 2-1. Performance of the micro fission chamber of ^{235}U.

Diameter	14 mm
Active length	76 mm
Fissile material	^{235}U 0.6 mg $(UO_2)/cm^2$ total 12 mg of UO_2
Ionizing gas	14.6 atm of Ar + 5% N_2
Housing material	Stainless steel 306L
Neutron sensitivity for fission reactor spectrum Pulse counting mode MSV mode DC mode	 2.2×10^{-3} cps/nv 5.7×10^{-28} A^2/Hz/nv 4.6×10^{-15} A/nv
Gamma sensitivity MSV mode DC mode	 7.72×10^{-29} A^2/Hz/R/h 1.54×10^{-12} A/R/h

2.2 Installation Position

In the ITER CDA (Conceptual Design Activity), we planned to install micro fission chambers just under the first wall. However, that is rather difficult because nuclear heating will be more than 10 W/cc, and burn-up of the fissile material will reduce the life-time of the detector. In order to find suitable detector positions around the shield blanket modules and to determine the best fissile material, we carried out neutronics calculations using the two-dimensional neutron transport code DOT 3.5. Figure 2-3 shows the slab model for the calculation. The model includes the first wall, the shielding blanket, with a gap between adjacent modules, the back plate, and the vacuum vessel.

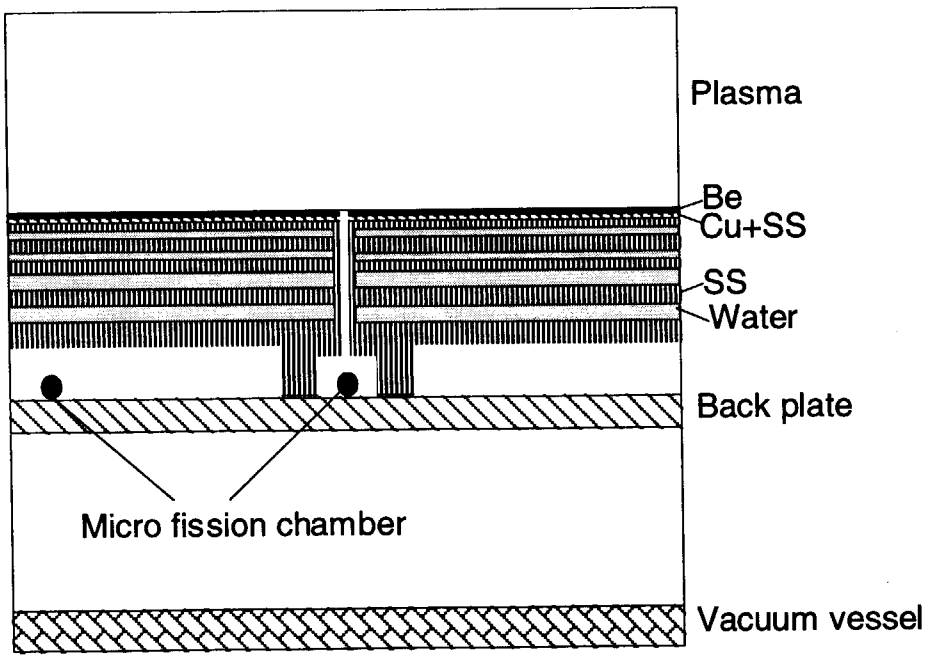

Fig. 2-3. Model for two dimensional neutron calculation using DOT 3.5 code. The model includes the first wall, shielding blanket with gap between adjacent modules, back plate of blankets and vacuum vessel.

Figure 2-4 shows the distributions of neutron and gamma flux and nuclear heating rate for stainless steel along the radial direction in the shielding blanket. The flux of 14 MeV neutrons decreases 10^3 by the blanket. However, total neutron and gamma fluxes decrease 10^2 and ~50, respectively. The neutron spectra on the surface on the Be first wall, center the blanket module, front and rear surfaces of the back plate are shown in Fig.2-5. Those spectra have almost same shape except 14 MeV component. From the engineering point of view, installation of a detector inside the shielding blanket is difficult because of the extremely tight space among cooling channels. The best candidate positions for detector installation are in the gap between adjacent blankets modules and behind the blanket on the back plate. Figure 2-6 shows neutron and gamma spectra for those two positions. The neutron flux in the gap is about 10 times larger than that behind the blanket. On the other hand, the gamma flux in the gap is only three times larger.

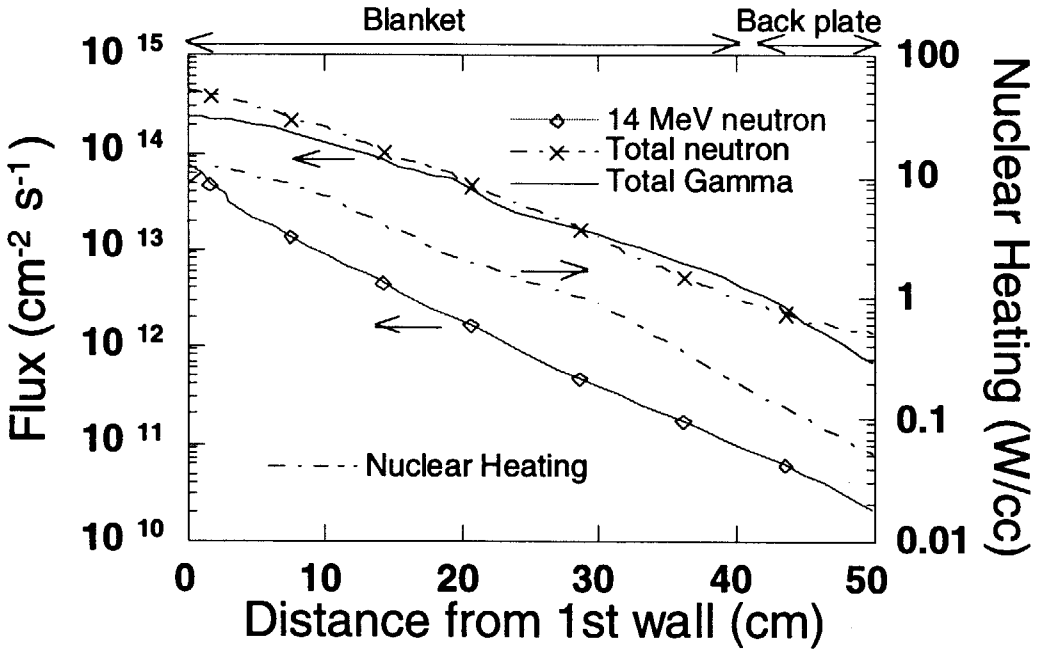

Fig. 2-4. Distributions of neutron and gamma flux, and nuclear heating rate for stainless steel along the radial direction in the shielding blanket.

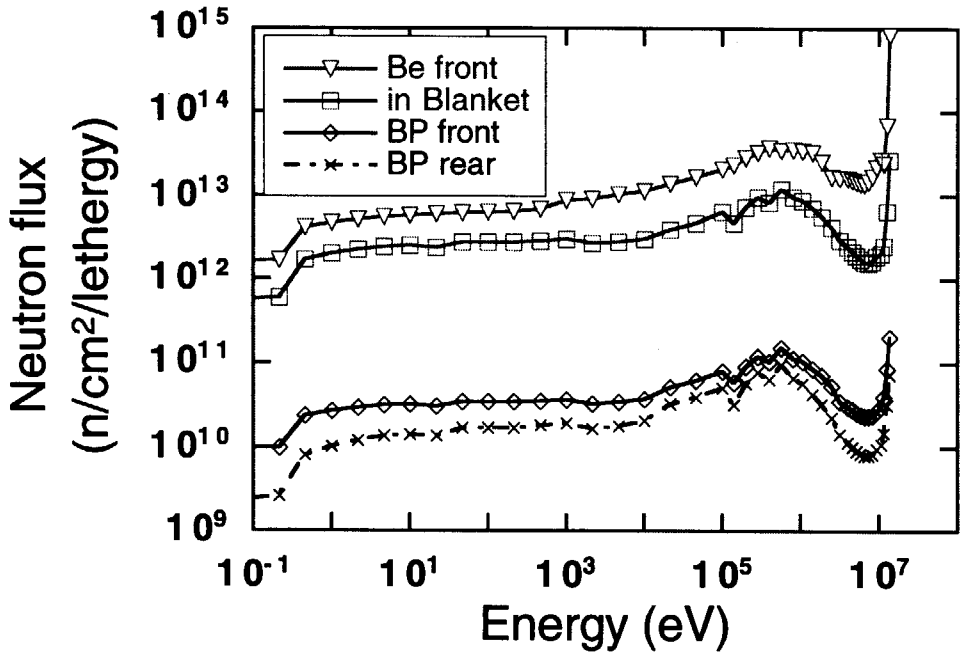

Fig. 2-5. Neutron spectra on the surface on the Be first wall(Be front), center the blanket module (in Blanket), front(BP front) and rear surfaces of the back plate(BP rear).

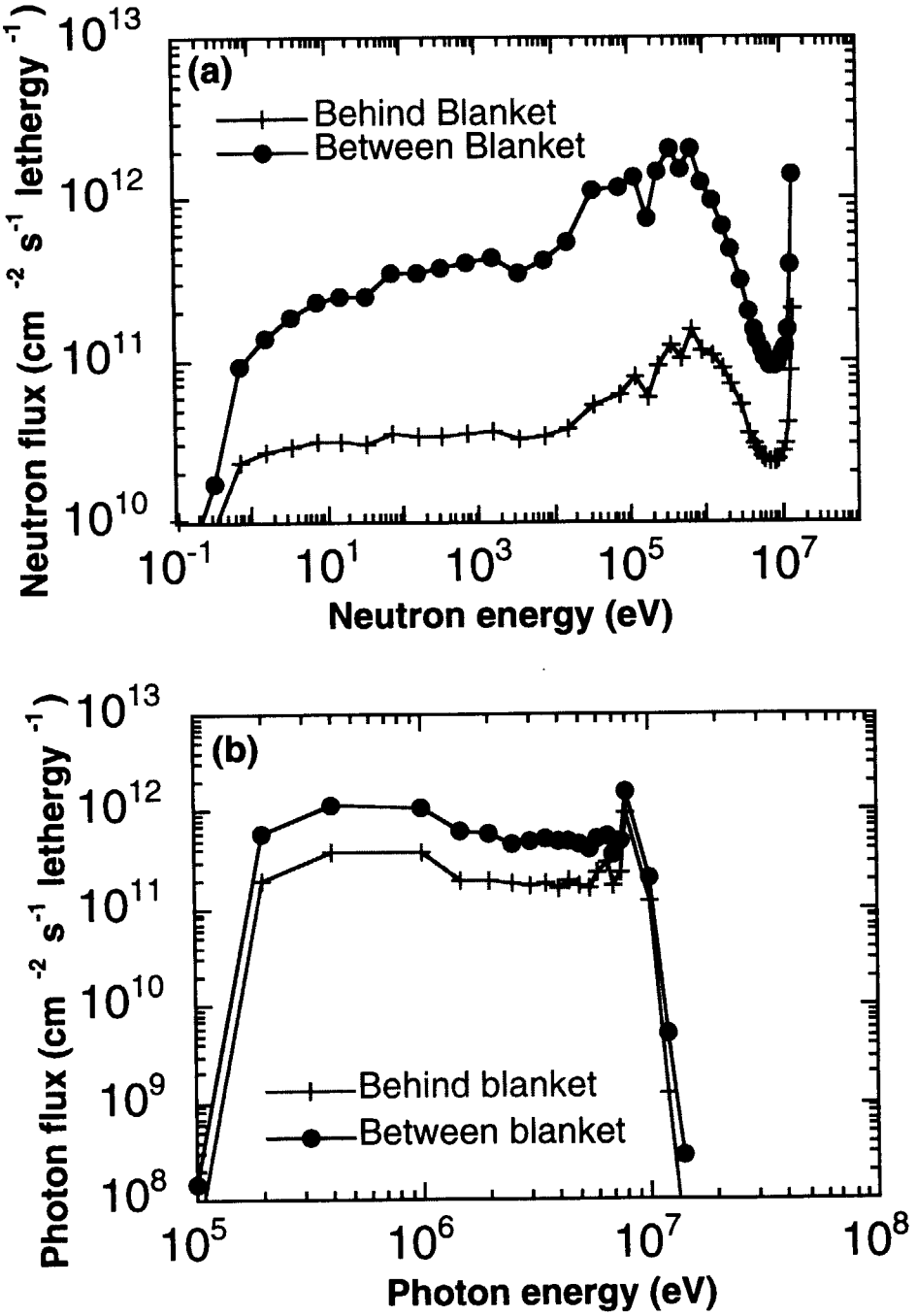

Fig. 2-6. Neutron(a) and gamma spectra(b) in the gap between the adjacent and behind the blanket on the back plate.

Total neutron and gamma flux, and expected fission reaction rates of ^{235}U and ^{238}U are listed in Table 2-2 for micro fission chambers with 10 mg uranium in a nominal 1.5 GW ITER plasma. In order to get wide dynamic range, the fission reaction rate during maximum power operation of ITER should be as high as the operational limit of the detector. The maximum fission reaction rate of this type of

chamber is 10^{10} s^{-1} for the Campbelling mode. Therefore, a ^{235}U chamber may be used both behind the blanket and in the gap. A ^{238}U chamber has is suitable for use only in the gap.

Table 2-2. Fission reaction rates in ^{235}U and ^{238}U micro fission chambers.

	Behind blanket	In gap
Total neutron flux (cm^{-2} s^{-1})	9.0×10^{11}	9.7×10^{12}
Total gamma flux (cm^{-2} s^{-1})	1.2×10^{12}	3.5×10^{12}
Fission reaction rate: ^{235}U (s^{-1})	9.9×10^{8}	2.3×10^{9}
Fission reaction rate: ^{238}U (s^{-1})	2.3×10^{6}	1.7×10^{7}
Nuclear heating (W/cc)	~0.05	~0.5

2.3 Life Time

We have to take the change of the sensitivity of the chamber due to the burn-up of the fissile material into account. ^{235}U is burned up through mainly fission and neutron capture reactions. So the number of ^{235}U atoms N_{235U} is represented by following equation;

$$\frac{d}{dt}N235U(t) = -N235U(t)\phi(\sigma_{f235U} + \sigma_{C235U}) \tag{2-1}$$

where σ_{f235U} and σ_{C235U} are averaged fission and neutron capture cross-sections defined by

$$\sigma = \frac{\int \sigma(E)\phi(E)dE}{\int \phi(E)dE} \tag{2-2}$$

where $\phi(E)$ is the neutron energy spectrum at the micro fission chamber. Figure 2-7 shows cross-sections of fission, neutron capture and other reactions for ^{235}U. From equation (2-1),

$$N_{235U}(t) = N_{235U}(0)Exp\{-\phi(\sigma_{f235U} + \sigma_{C235U})t\} \tag{2-3}$$

is obtained. In the gap, $\phi\sigma_{f235U}$ and $\phi\sigma_{C235U}$ are 7.1×10^{-11} s^{-1} and 5.3×10^{-13} s^{-1}, respectively for the 1.5 GW operation. So the fission reaction is dominant. The sensitivity S_{235U} is represented by

$$S_{235U} = N_{235U}\,\phi\,\sigma_{f235U} \tag{2-4}$$

The change of the sensitivity is evaluated to be only 0.1 % and 0.2 % behind blankets and in the gap, respectively, during the ITER life-time of 1.5 GW•year. Therefore, we can use ^{235}U chambers without replacement.

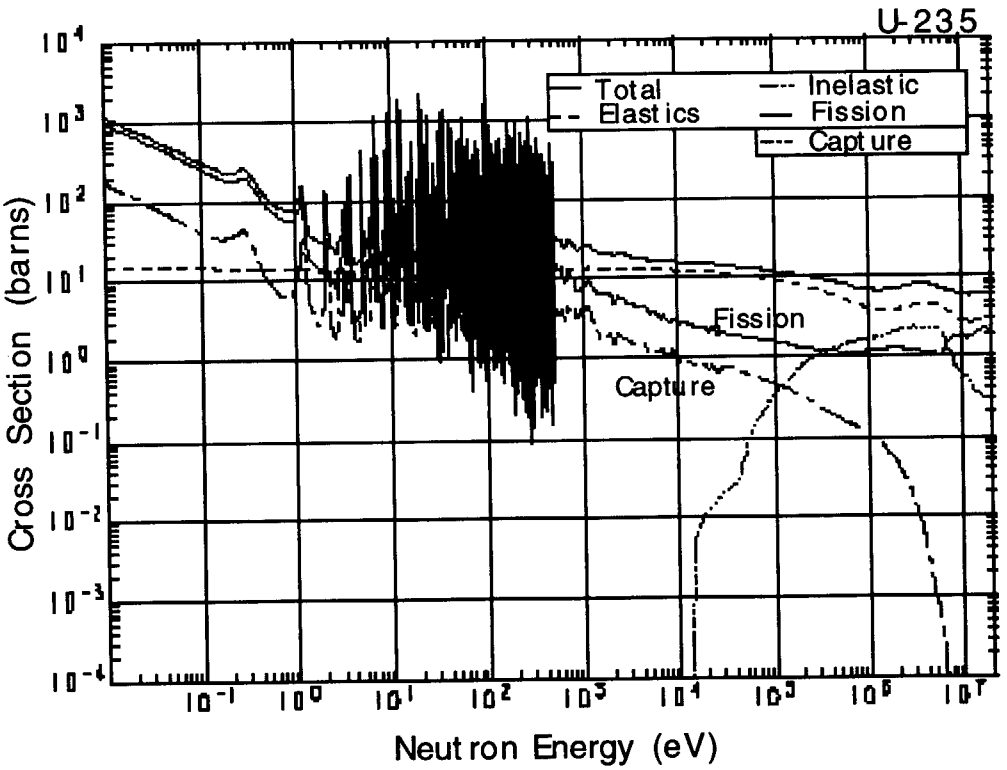

Fig. 2-7. Neutron cross-section of ^{235}U from JENDL 3.2[10].

Burn-up of ^{238}U is much more complicated.It occures mainly by neutron capture in the thermal energy range, which produces ^{239}Pu via following chain;

$$^{238}U + n \rightarrow {}^{239}U + \gamma$$

$$^{239}U \rightarrow {}^{239}Np + \beta$$

$$^{239}Np \rightarrow {}^{239}Pu + \beta\,. \qquad (2\text{-}5)$$

The detection efficiency of the ^{238}U chamber may increase due to buildup of ^{239}Pu, which has a large fission cross-section for thermal neutrons. the numbers of ^{238}U and ^{239}Pu atoms are represented by following equation;

$$\frac{d}{dt}N238U(t) = -N238U(t)\phi(\sigma_{f238U} + \sigma_{C238U}) \qquad (2\text{-}6)$$

$$\frac{d}{dt}N239Pu(t) = N238U(t)\phi\sigma_{C238U} - N239Pu(t)\phi(\sigma_{f239Pu} + \sigma_{C239Pu}) \qquad (2\text{-}7)$$

Figures 2-8 and 2-9 show cross-sections of fission, neutron capture and other reactions for ^{235}U and ^{239}Pu.

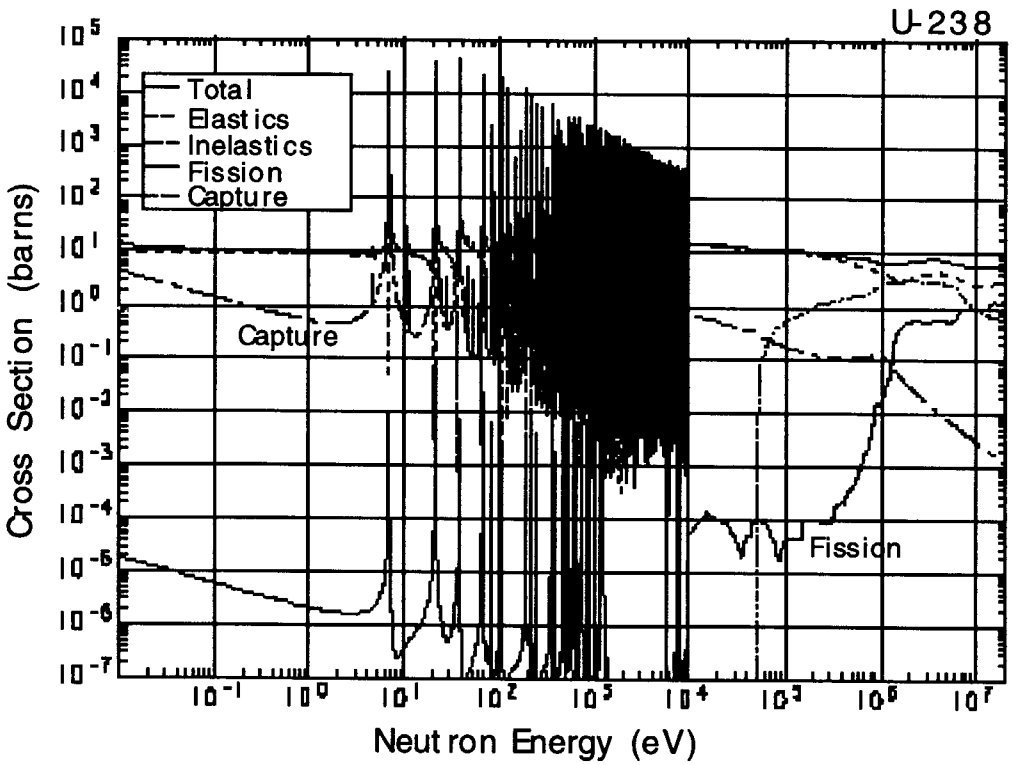

Fig. 2-8. Neutron cross-section of ^{238}U from JENDL 3.2[10].

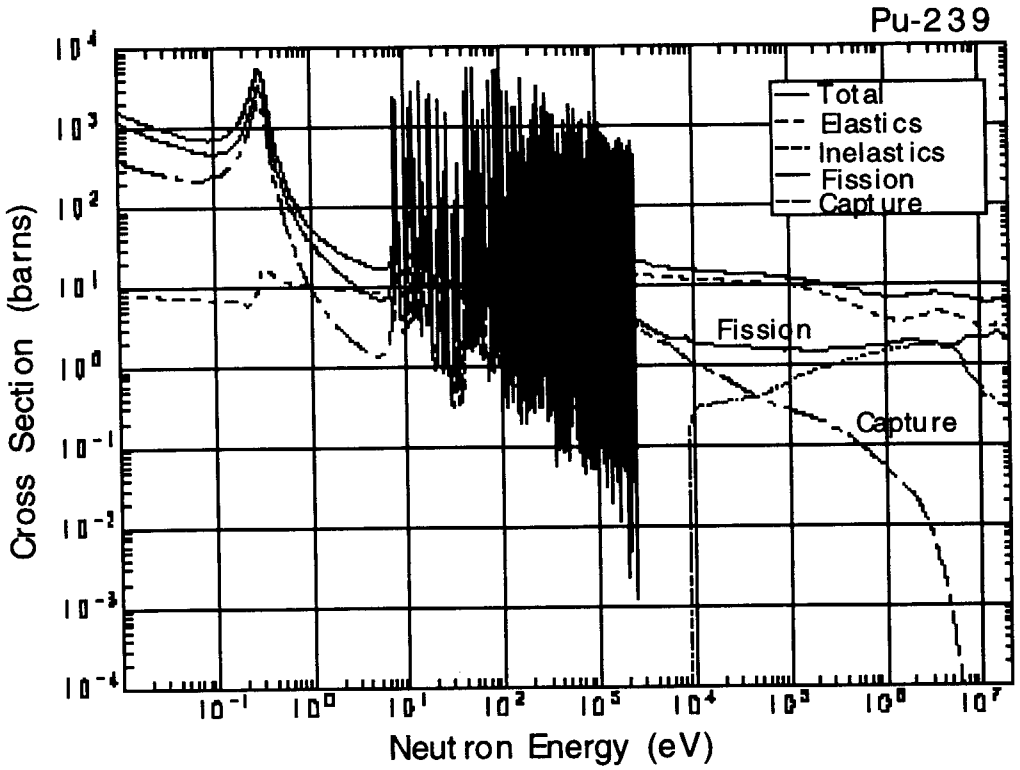

Fig. 2-9. Neutron cross-section of ^{239}Pu from JENDL 3.2[10].

The neutron capture reaction is dominant process in the burn-up of ^{238}U. Within the ITER life time, the numbers of ^{238}U and ^{239}Pu atoms are given by,

$$N_{238U}(t) = N_{238U}(0)\ (1-\phi\sigma_{C238U}t) \tag{2-8}$$

$$N_{239Pu}(t) = N_{238U}(0)\ \phi\sigma_{C238U}t \tag{2-9}$$

The sensitivity of the 238U micro fission chamber S_{238U} is represented by

$$S_{235U} = N_{238U}\,\phi\,\sigma_{f238U} + N_{239Pu}\,\phi\,\sigma_{f239Pu} \tag{2-10}$$

After the 1.5 GW•year operation, the burn-up of ^{238}U is only 0.2 %, but the detection efficiency will increase 50 % due to accumulation of ^{239}Pu. Unless this change is properly accounted for, it is too large to allow use of ^{238}U chambers as neutron monitors in ITER.

2.4 Gamma-ray Effect

This type of micro fission chamber can be operated in the pulse counting, Campbelling, and current modes. We have evaluated the noise due to gammas for those three operation modes.

In the pulse counting mode, the current pulse generated by fission fragments or by gamma reactions in the ionizing gas is measured. The fission reaction releases ~100 MeV as the kinetic energy of fission fragments. One fragment goes into the ionization gas and another goes into electrode wall. Averaged energy deposited in the ionization gas is about 43 MeV, on the other hand gamma energy is less than 10 MeV (see Fig.2-6b). We can eliminate the gamma pulses by conventional pulse discrimination techniques. The Campbell mode sensitivity is given from the following formula,

$$I_{rms}^2 = N q^2 \int f^2(\omega) B(\omega) d\omega/\pi \quad (2\text{-}11)$$

where N is the fission reaction rate, q is electric charge generated by a fission reaction given by

$$q = 43 \text{ MeV}/26 \text{ eV} \times (1.6 \times 10^{-19} \text{ C}) \\ 2.7 \times 10^{-13} \text{ C}, \quad (2\text{-}12)$$

where 26 eV is the ionization energy of Argon gas. $f(\omega)$ is the frequency spectrum of the detector output, and $B(\omega)$ is the filter function of the amplifier, which is usually step function of 100 kHz-400 kHz. The gamma sensitivity in Campbelling mode is 7.7×10^{-29} $A^2/Hz/(R/h)$ for those chambers. The expected Campbell currents due to neutrons and gammas are listed in Table 2-3, here gamma dose rates are converted from the gamma spectra shown in Fig.2-6(b). We can neglect the gamma effects in Campbelling mode.

The current mode measures directly the ionization current in the fission chamber. Also we calculated the outputs in the current mode as shown in Table 2-3. The gamma sensitivity in current mode is 2.2×10^{-12} A/(R/h). In current mode it is too large to be neglected. We have discarded the use of current mode for unshielded micro fission chambers.

Table 2-3. Outputs of ^{235}U micro fission chamber by neutrons and gammas in Campbelling and current modes.

	Behind blanket	In gaps
Gamma dose rate (R/h)	3.5×10^{6}	8.6×10^{6}
Campbelling mode (A^2/Hz)		
Neutrons	2.3×10^{-17}	5.3×10^{-17}
Gammas	2.7×10^{-22}	6.6×10^{-22}
Current mode (A)		
Neutrons	2.6×10^{-4}	6.0×10^{-4}
Gammas	8.0×10^{-6}	1.9×10^{-5}

2.5 Dynamic Range

A dynamic range of 10^7 in a single fission chamber has been demonstrated in the JT-60U neutron monitor[3] with both pulse counting and Campbelling modes. This meets the ITER requirement for the neutron monitor. The linearity was calibrated before installation on JT-60U, using a fission reactor with output power range of 10^7 as shown in Fig. 2-10.

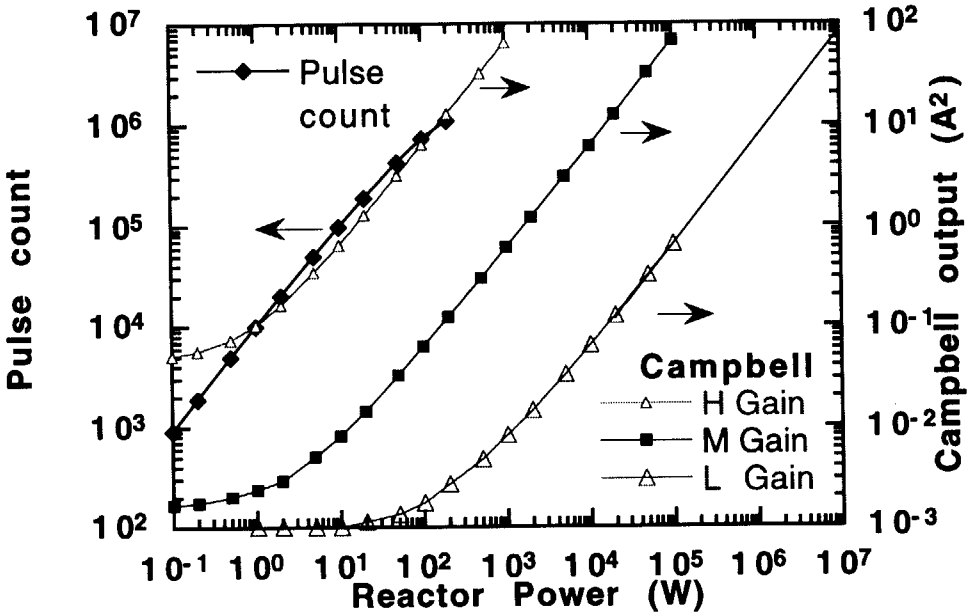

Fig. 2-10. Linearity calibration of the JT-60U fission chamber[3] using a fission reactor

We confirmed two decades of overlap in pulse counting and Campbelling modes. From this experience, we conclude that a micro fission chamber containing 10 mg of ^{235}U can cover the 10^7 range of ITER operation as shown in Fig. 2-11.

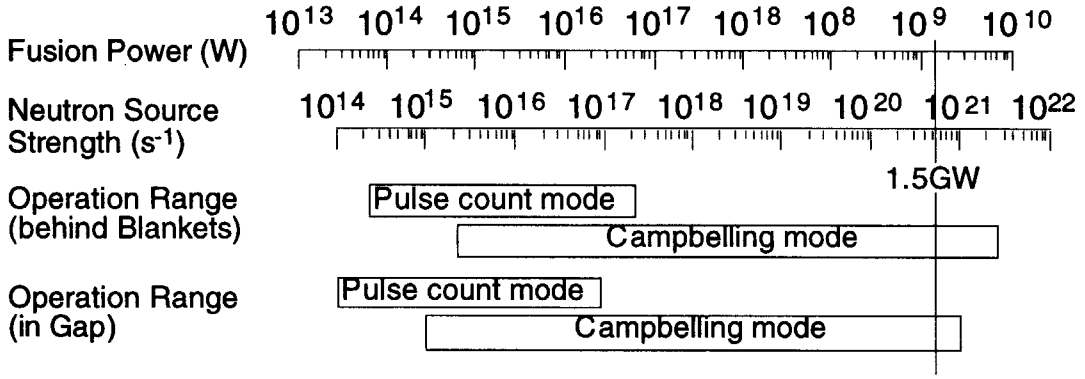

Fig. 2-11. Operation range of ^{235}U micro fission chambers behind blanket and in the gap of adjacent blankets.

2.6 Magnetic Field Effect

The effect of the strong magnetic field on the fission chamber is another problem. In the fission chamber, we measure the electron induce current from ionization by fission fragments. So we calculated the electron drift orbit in the magnetic field. The electron drift velocity **u** is represented by

$$\mathbf{u} = \frac{\mu_e}{1 + \omega_c^2/\nu^2}\left[\mathbf{E} + \frac{\mathbf{E}\times\mathbf{B}}{B}\frac{\omega_c}{\nu} + \frac{(\mathbf{E}\cdot\mathbf{B})}{B^2}\frac{\omega_c^2}{\nu^2}\right] \tag{2-13}$$

where m_e is the electron mobility, n is the collision frequency of the electron to neutral atoms, and w_c is the electron cyclotron frequency in the magnetic field **B**. If we assume $\mathbf{E} = (E_x, 0, 0)$ and $\mathbf{B} = (0, 0, B_z)$,

$$\mathbf{u} = \left(\frac{\mu_e E_x}{1 + \omega_c^2/\nu^2}, \frac{\mu_e E_x}{1 + \omega_c^2/\nu^2}\frac{\omega_c}{\nu}, 0\right) \tag{2-14}$$

As shown in Fig.2-12, an angle between **u** and **E**, Lorentz angle α, is represented by $\tan\alpha = \omega_c/\nu$. In the case of the micro fission chamber with 14.6 atm Argon gas, applied voltage of 200 V to 0.5 mm electrode gap, in the magnetic field of 5.7 T, the mobility without magnetic field is $u_0 \approx 3 \times 10^3$ m/s. the Lorentz angle is evaluated as,

$$\tan\alpha = \frac{\omega_c}{\nu} \approx \frac{B}{E} u_0 = 0.04 << 1 \qquad (2\text{-}15)$$

Thus the magnetic effect on the electron drift velocity is to be negligible. However, we do not have experience of a fission chamber using in high magnetic field such as 5.7T. We should confirm the magnetic effects on the fission chamber experimentally.

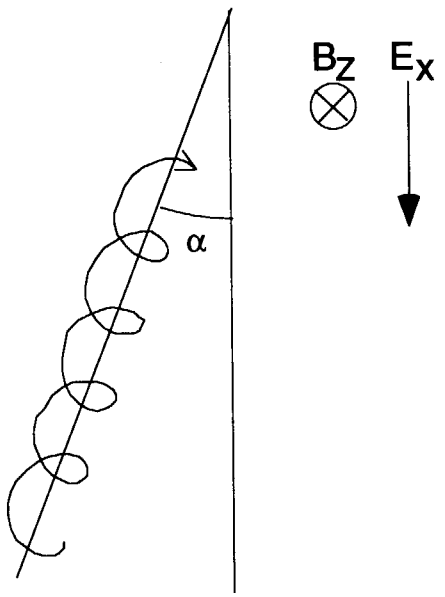

Fig. 2-12. Lorentz angle of electron drift in magnetic field.

2.7 Nuclear Heating

Nuclear heating of the detector is an important issue for the invessel diagnostics. Active water cooling the detector is rather difficult due to the tight space between the blanket modules and back plate. Figure 2-13 shows distributions of the nuclear heating rate of the back plate along the poloidal gap of the blanket modules. Major material of the micro fission chamber is stainless steel same as the back plate, so that the nuclear heating is almost same. The nuclear heating is approximately 0.7 and 0.5 W/cc in the gap and behind the blanket module, respectively, except near the corner.

The micro fission chamber can be operated in the temperature up to 300 °C, so that it seems possible to cool it by thermal contact with the back plate which cooled by water. Also in the instrumentation divertor cassette, the nuclear heating is less than 0.5 W/cc except the dome and target plates as shown in Fig.2-14.

Moderator such as polyethylene surrounding the detector is desired to get flat energy response in wide energy range. Polyethylene moderator shield could not be used due to the nuclear heating. If the polyethylene can survive in the high temperature, the fission chamber will be baked up due to nuclear heating because the polyethylene is thermal insulator. So we gave up the moderator.

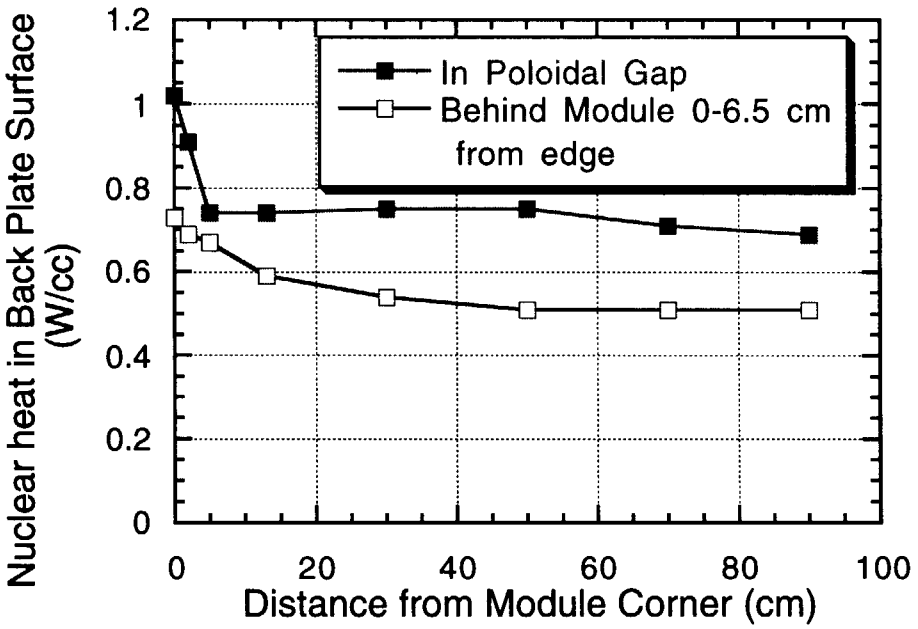

Fig. 2-13. Distribution of the nuclear heating rate of the back plate along the poloidal gap of the blanket modules.

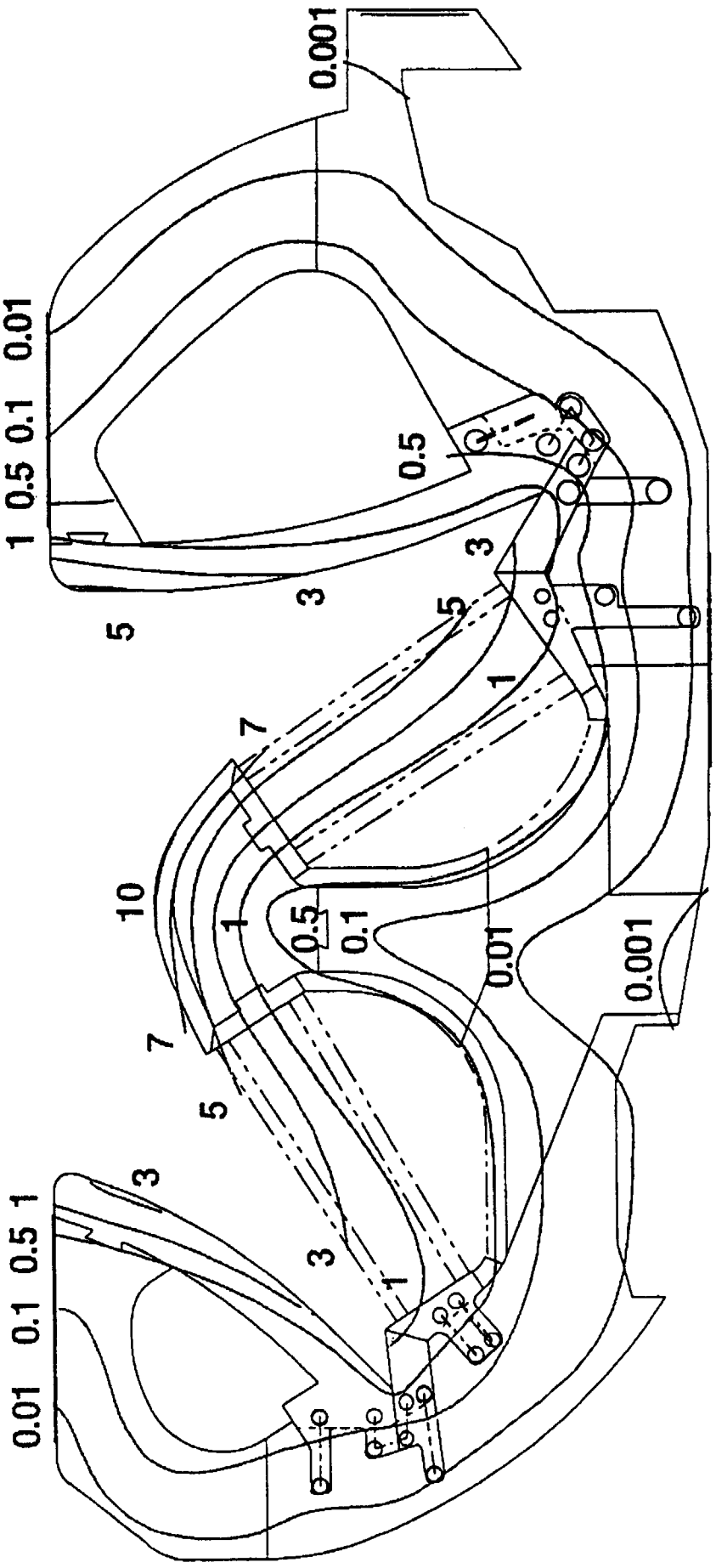

Fig. 2-14. Neuclear heating distribution in the blanket module. Values are in W/cm3. The nuclear heating is less than 0.5 W/cc except the dome and target plates.

2.8 Effects of Plasma Position and Neutron Source Profile

The detection efficiency of a neutron detector inside the vacuum vessel will be affected by changes in the plasma position and the neutron source profile. However, we can reject or reduce the effects by installing the detectors at several poloidal angles.

We have investigated the responses of the micro fission chambers by a neutron Monte Carlo calculations using the MCNP version 4A code. An 18-degree sector of the first wall, shielding blanket, blanket back plates and vacuum vessel are modeled by a simple torus with elliptic cross-section as shown in Fig. 2-15. The divertor cassettes, ports and coils are not included. Only one poloidal gap between adjacent blanket modules is modeled. We use the neutron cross-section set based on JENDL 3.2.

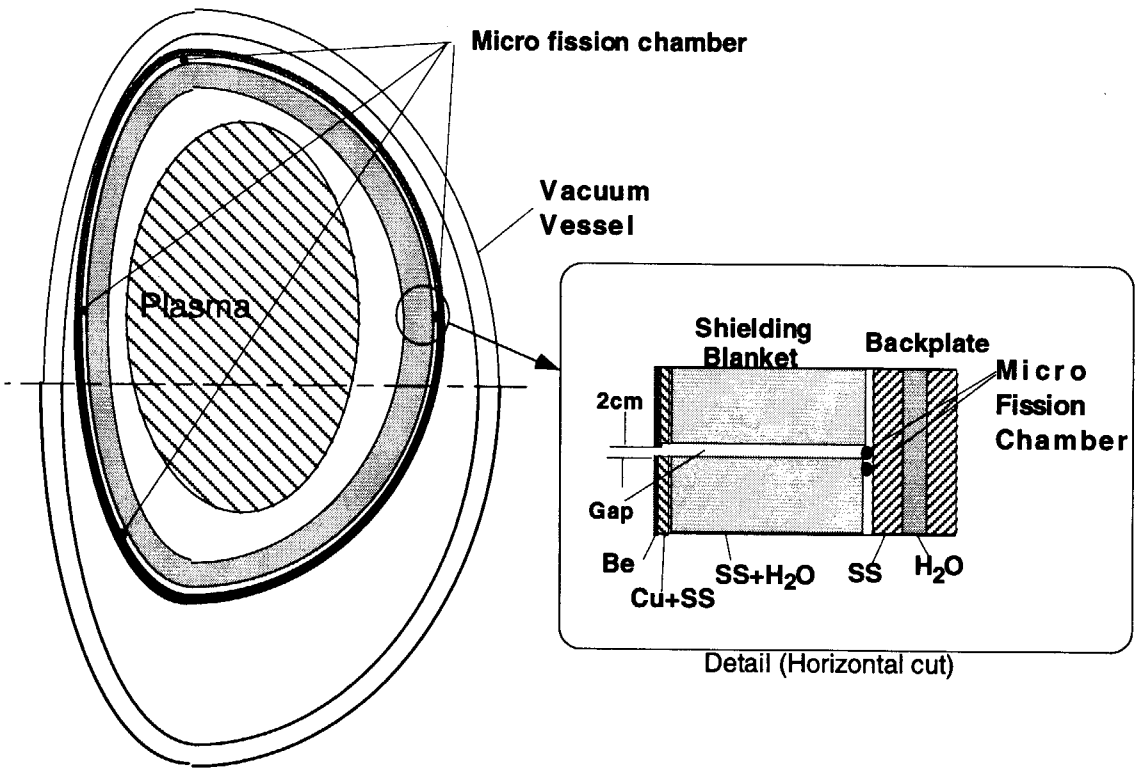

Fig. 2-15. Model for a neutron Monte Carlo calculation. 18 degree sector of the first wall, shielding blanket, blanket back plate, and vacuum vessel are modeled by a simple torus with elliptic cross-section.

The neutron source is toroidally symmetric with 14 MeV monoenergetic energy. The source has a poloidal distribution given by

$$S = \left[1 - \left\{ \frac{(R-R_P)^2}{a_p^2} + \frac{(Z-Z_P)^2}{a_p^2 \kappa^2} \right\} \right]^m , \tag{2-16}$$

where R_P is the major radius, a_P is the minor radius, Z_P is the vertical shift of the plasma center, κ is the ellipticity, and m is the power of the parabolic profile. The angular emission is isotropic. The reference parameters are R_P = 8.14 m, a_P = 2.3 m, Z_P = 1.4 m, κ = 1.6 and m = 0.8. In this case, the neutron source peaking factor is represented by

$$\frac{S_n(0)}{\langle S_n \rangle} = m + 1 \tag{2-17}$$

where $S_n(o)$ and $<S_n>$ are the central and volume averaged neutron emissivity, respectively.

We calculated the detection efficiencies of the ^{235}U micro fission chambers at typical 4 poloidal positions in the gap as shown in Fig.2-15. We have not obtained sufficient statistics for those behind the blanket. Figures 2-16 and -17 show the plasma position dependence of the detection efficiencies. For a horizontal shift of plasma position in the range ± 50 cm, the detection efficiency of the bottom detector is almost constant. The efficiency of the outside detector increases only 1.5 % with 50 cm increase in horizontal plasma position, while efficiencies of the inside and top detectors decrease 12 % and 3%, respectively. For a vertical shift of plasma position in the range ± 50 cm, detection efficiencies of the inside and outside detectors are almost constant. The top detector increases in efficiency by 8 % for a 50 cm increase in vertical plasma position while the bottom one decreases by 18 %.

Reference value of m = 0.8 is obtained by fitting of the neutron source profile derived from the reference of ion temperature. Figure 2-18 shows the neutron source profiles used in the MCNP calculations. The neutron source profile dependence of the detection efficiencies is shown in Fig.2-19. Both detection efficiencies of inside and outside detectors increase 10 % with the increase in the peaking factor of the neutron source profile from 1.8 to 3. However, those of top and bottom detectors are less sensitive to the peaking factor. Inside and outside detectors are so close to the plasma that those are easy to be affected by the plasma position and/or neutron source profile. We can reduce those effects by combining the outputs of different detectors. For example, the average of top and bottom detector signals is relatively insensitive to changes in plasma position.

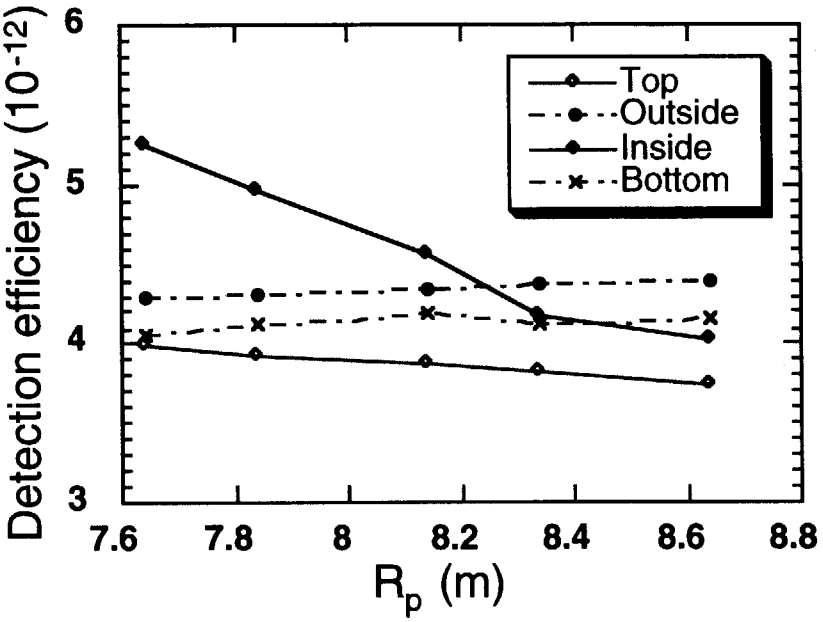

Fig. 2-16. Dependence of the detection efficiencies for the horizontal shift of the plasma position.

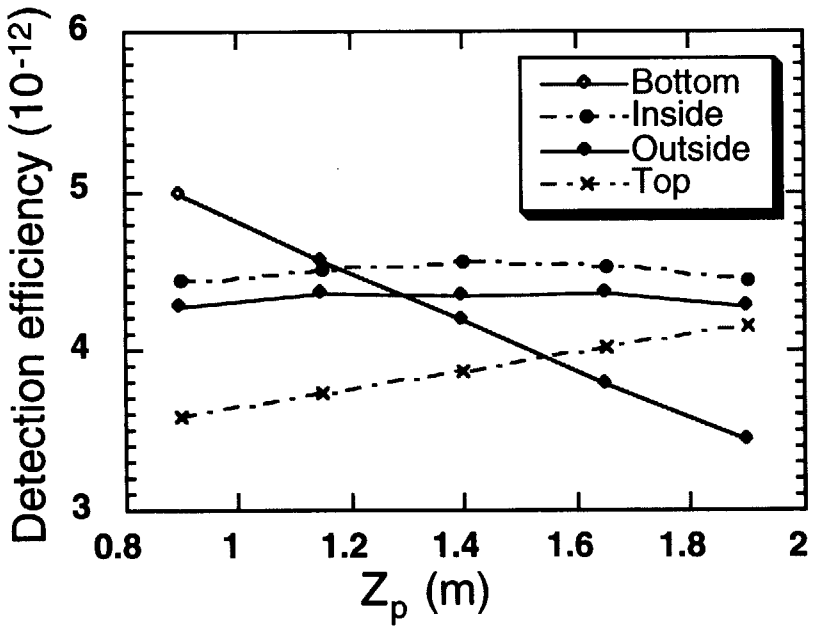

Fig. 2-17. Dependence of the detection efficiencies for the vertical shift of the plasma position.

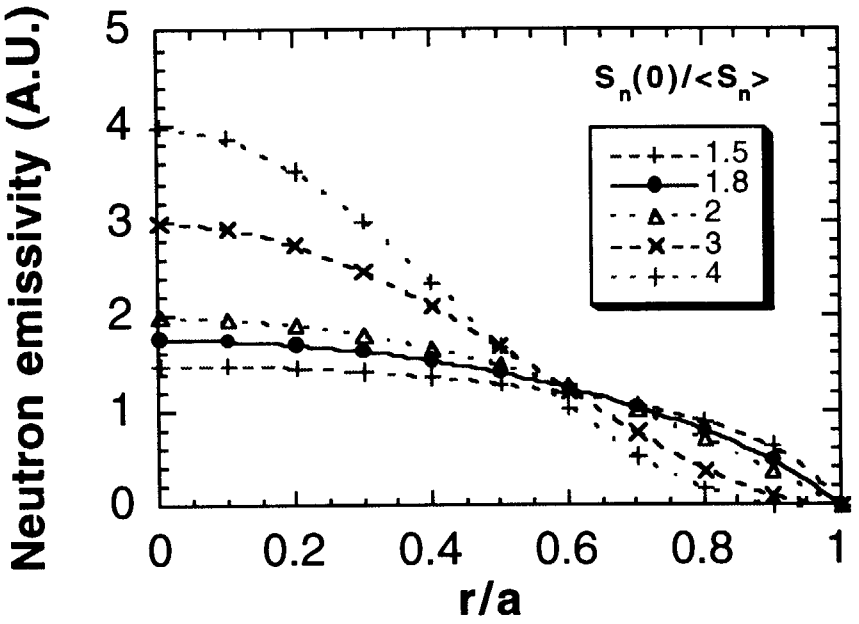

Fig. 2-18. Neutron source profiles with deferent peaking factor for MCNP calculations.

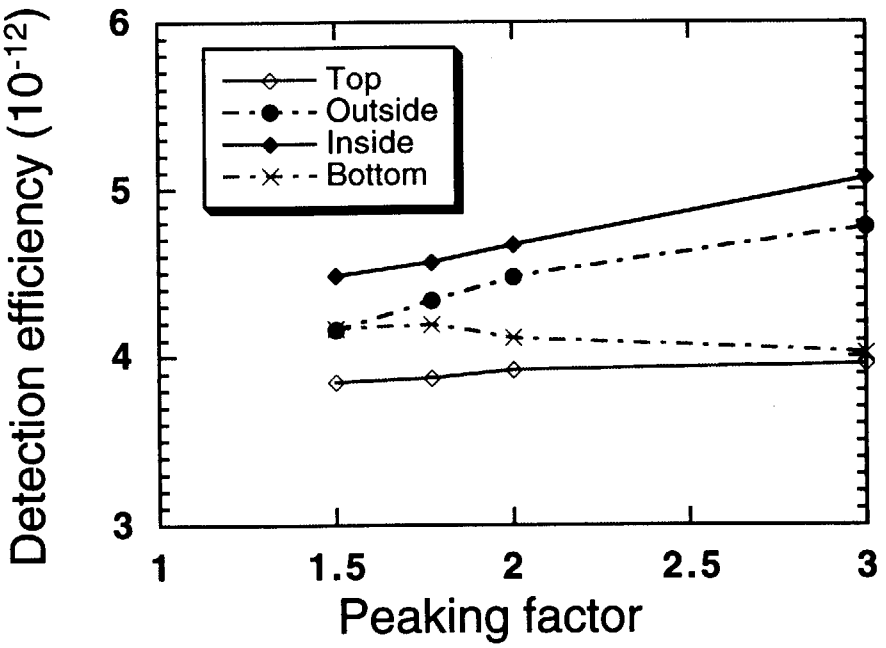

Fig. 2-19 Neutron source peaking factor dependence of the detection efficiencies.

2.9 Calibration

Absolute calibration of the fission chambers is one of the most critical issues in the design of the neutron source strength monitor system. In present tokamaks, neutron monitors are calibrated by measuring their response to a neutron source, such as a ^{252}Cf radioactive source or a DT neutron generator, placed at various positions inside the vacuum vessel.

We simulate the *in-situ* calibration by MCNP calculation, where a point neutron source is moving on the plasma axis as shown in Fig. 2-20. The modeling of ITER machine is same as in Fig.2-15.

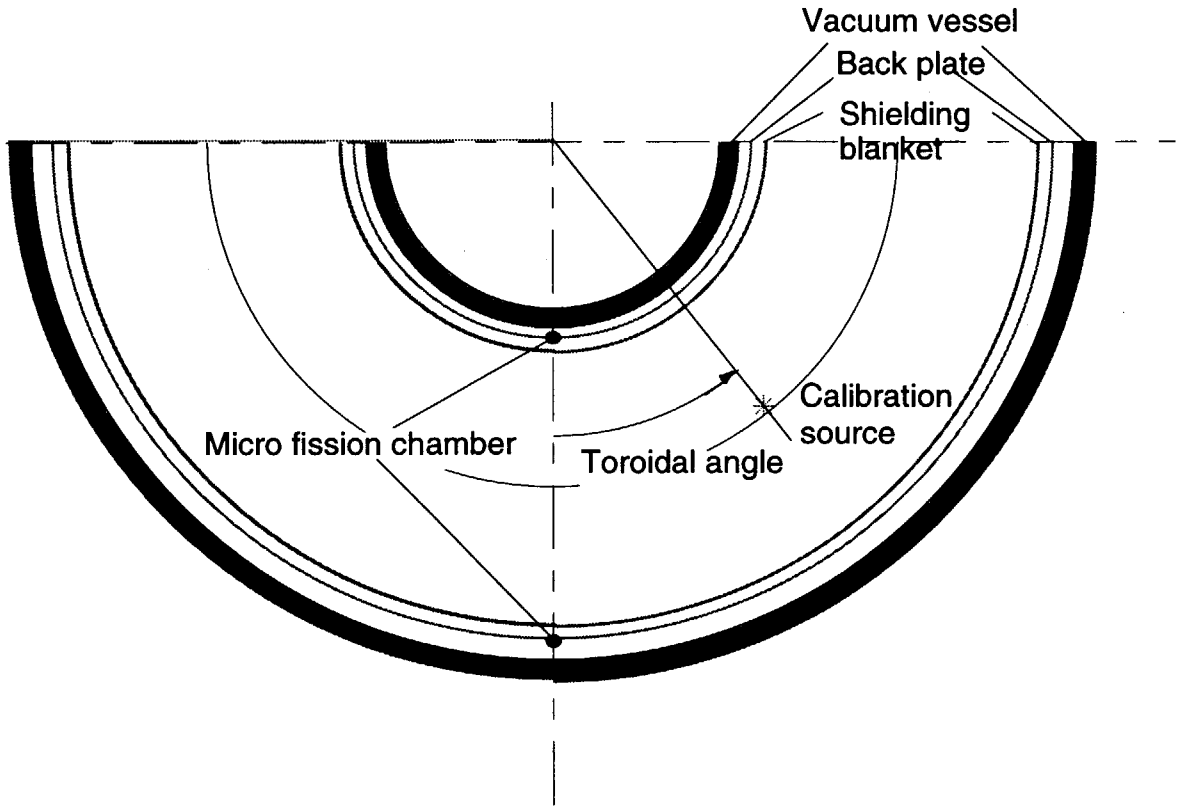

Fig. 2-20. Model of the *in-situ* calibration. A point neutron source is moving on the plasma axis

Figure 2-21 shows the detection efficiency of the detector in the gap (outside) for the point source on the plasma axis with R = 8.14 m plotted against the toroidal angle of the source. The response function is so highly peaked at toroidal angle of 0°, like δ function, that the total efficiency for the neutron source strength may be affected by the change of the gap width due to thermal expansion or magnetic stress. The issue is still open in the design work.

We need DT neutron generator with emission rate of ~10^{10} neutrons/s to get sufficient counting rate at *in-situ* calibration. We should develop such intense neutron generator which is movable by the standard remote handling apparatus.

Even if a neutron generator with an intensity of ~10^{10} neutrons/s is available, the count rate of a micro fission chamber will not be very high. Therefore, a high sensitivity, regular size fission chamber is desired for the calibration. We do not have space between the blanket module and back plate , so that the detector is proposed to be installed between the back plate and vacuum vessel. Now it is considered to mount it on the flame of the diamagnetic loop outside of the back plate. The micro fission chambers can be cross-calibrated by this high sensitive detector in DD or low power DT plasma operations.

In this design, micro fission chambers are operated mainly in Campbelling mode with wide dynamic range. Here the linearity calibration of the Campbelling output is necessary before the installation. As carried out in JT-60U(See Section 2.0-5), the linearity calibration using a fission reactor is proposed for this micro fission chambers.

By those calibrations, the micro fission chamber system hopefully can meet the required 10% accuracy goals of the fusion power measurement for the ITER project.

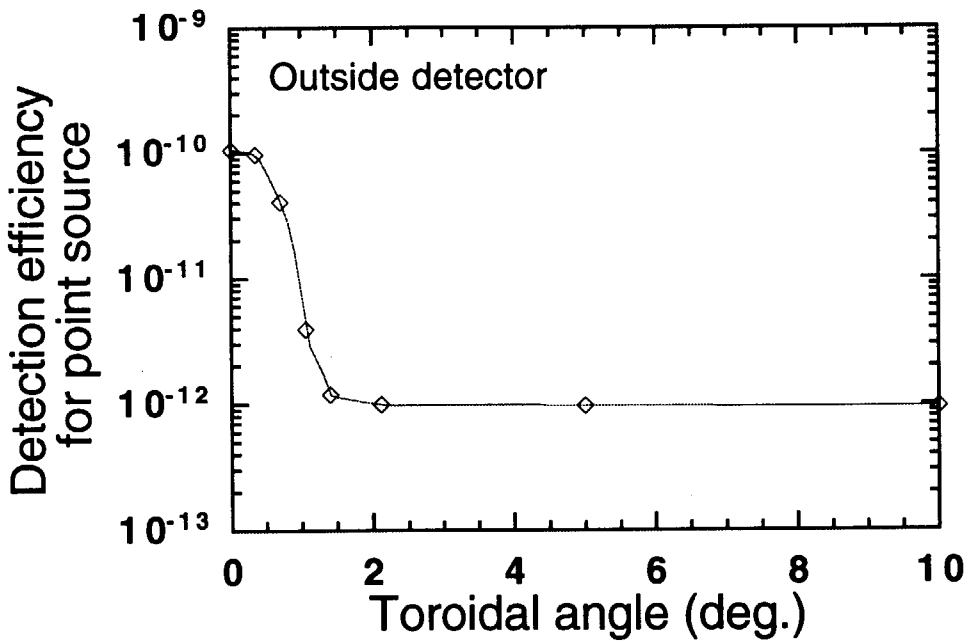

Fig. 2-21. Detection efficiency of outside detector for the point source on the plasma axis with R = 8.14 m plotted against the toroidal angle of the source.

3. DETAILED SYSTEM DESCRIPTION

3.1 General Equipment Arrangement

The micro fission chamber system should be operational for the entire ITER life-time. Since detector replacement will be difficult, we would like to install enough micro fission chambers to allow the system to continue functioning if some of the detectors fail. Figure 3-1 shows the proposed arrangement of micro fission chambers on ITER. Ten pairs of ^{235}U chambers are installed at 10 poloidal locations in one toroidal location. Each poloidal location has a pair of detectors. One chamber is behind a blanket module and another is in the gap–between adjacent blanket modules at each poloidal location. Another chamber is installed in the divertor cassette just under the dome.

We have two toroidal location for the poloidal detectors and four divertor cassette for the divertor detector as shown in Fig. 3-2. Additionally, a couple of the high sensitive detectors are installed for *in-situ* calibration purpose. So the total 44 micro fission chambers and two normal size fission chambers are proposed. According to the calibration detectors, neutron flux monitors has similar concept detectors, it is possible to shear them. As described in Section 2.0.9, the effect of the changes in the gap width due to thermal expansion etc. is not evaluated yet. If the effect is not negligible, we have to give up the detectors in the gap. From the cost saving point of view, it is possible that half of the detectors are connected to the electronic, and another half is stand-by without electronics for trouble.

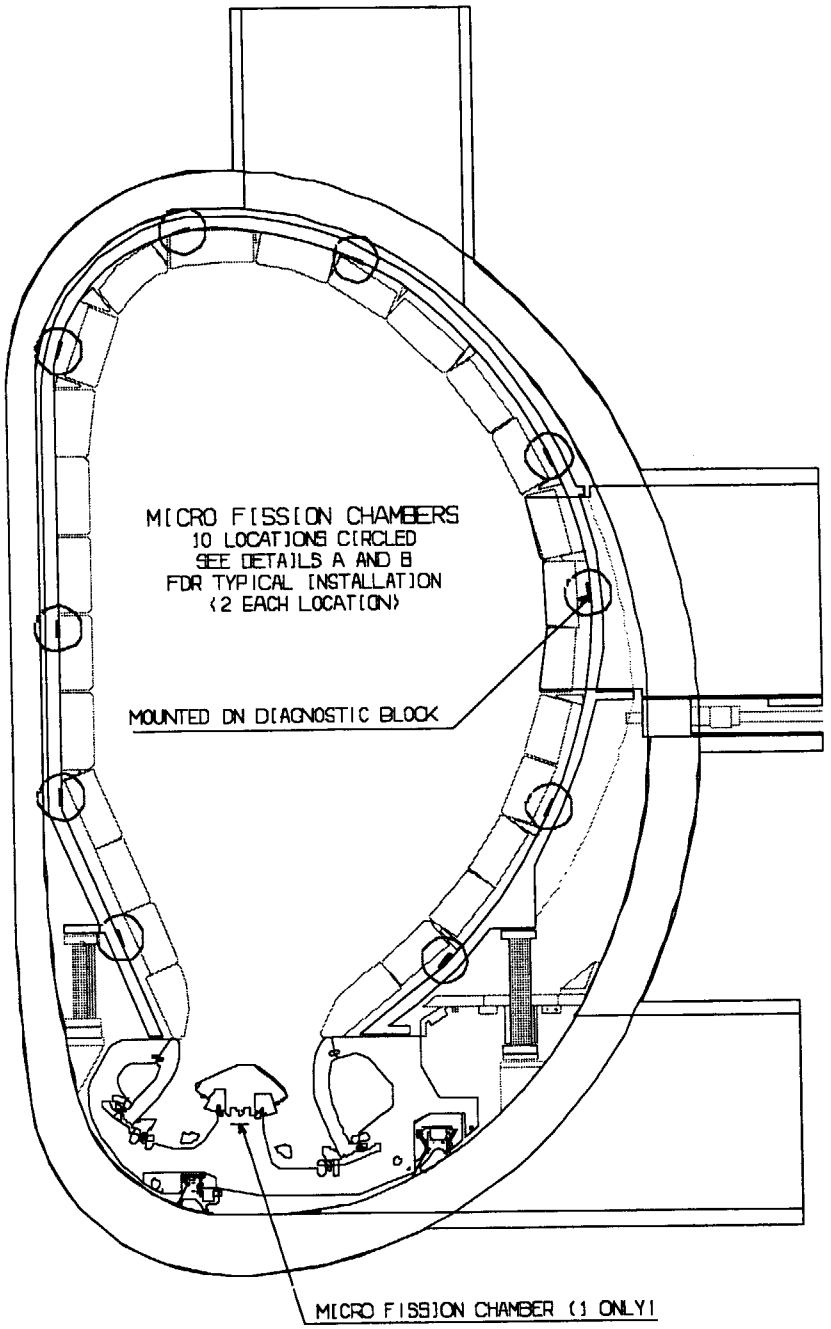

Fig. 3-2. Arrangement of micro fission chambers. Ten pairs of ^{235}U chambers are installed at 10 poloidal locations in a toroidal location. One chamber is installed in the divertor cassette just under the dome.

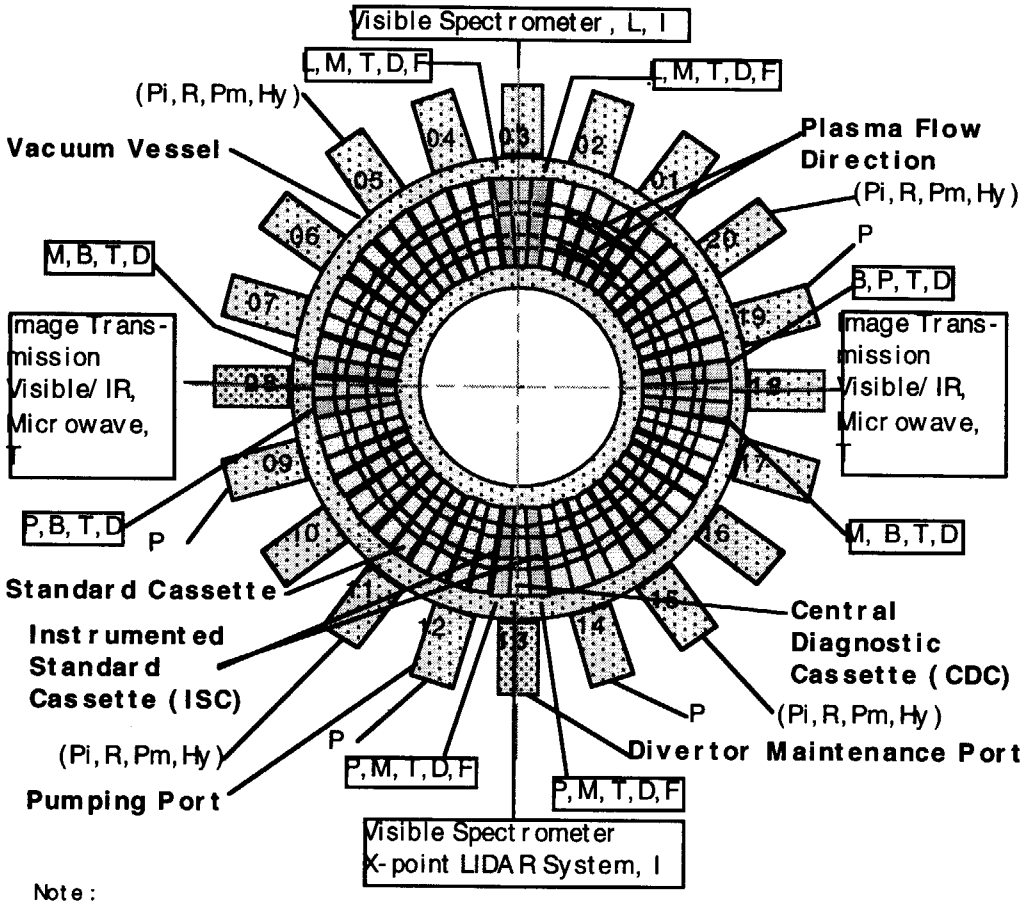

Note :
Instrumentation in frames is mounted on cassettes.
Instrumentation without frames is installed inside divertor ports.

VUV spectrometer is allocated to pumping ports (No. is TBD).

Magnetics on structure are mounted on the back plate of vacuum vessel.

Instrumentation in ISCs at ports 8 & 18 is half set.

Pi, R, Hy and Pm are allocated to four pumping ports as part of the monitor of divertor pumping sysytem (TBD).

Notation :
P : Pressure Gauge (ASDEX Gauge)
M : Magnetic Pickup Coil
B : Bolometer
L : Langmuir Probe
T : Thermocouple
H : Magnetics on Structure (Halo Current Sensor)
D : Deformation Gauge
F : Micro Fission Chamber
I : Impurity Implants
Pi : Pressure Gauge (Wide Range Vacuum Gauge)
R : RGA
Pm : Pressure Meter
Hy : Hydrogen Monitor

Fig. 3-2. Allocation of micro fission chamber and other instruments in the divertor cassette.

3.2 Arrangement on Back Plate

Figure 3-3 shows the isometric view of the micro fission chambers on the back plate. One chamber is behind a blanket module and another is in the gap-between adjacent blanket modules at each poloidal location. The detectors are mounted tightly on the diagnostics socket, the back surface of which faces water coolant inside the back plate. The outer sheath of the detector is electrically connected to the socket. However, the housing of the detector is maintained at the same ground level as the amplifier.

The output signal is transferred via the same MI cable as the high voltage supply. The cables are routed through generic diagnostics conduits, pass through the back plate. Those cables pass through the back plate and go out via a divertor pumping port. At the vacuum boundary, those cables are connected by a multi-wire coaxial connector.

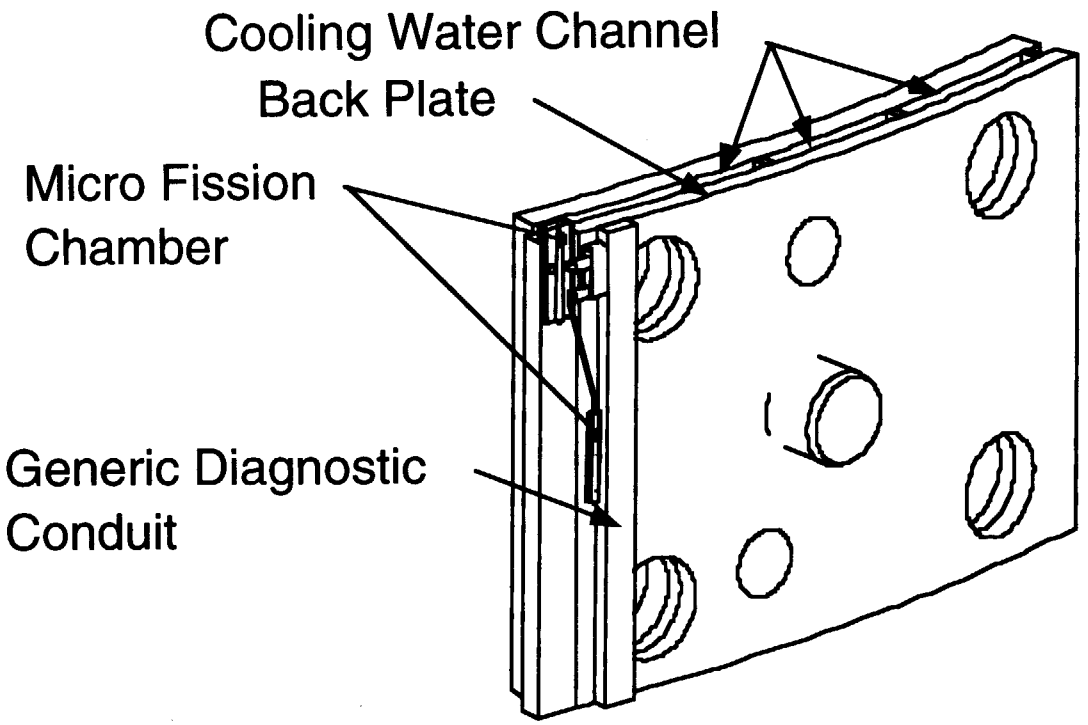

Fig. 3-3 Isometric view of the micro fission chambers on the back plate.

3.3 Arrangement in Divertor Cassette

Figure 3-4 shows the arrangement of the micro fission chamber in the divertor cassette. Other diagnostics sensors, such as bolometers and Langmuir probes, are installed in the same cassette (instrumentation divertor cassette). One micro fission chamber is placed under the dome, oriented horizontally, and is mounted tightly on the sensor panel of the divertor cassette as shown in Fig. 3-5

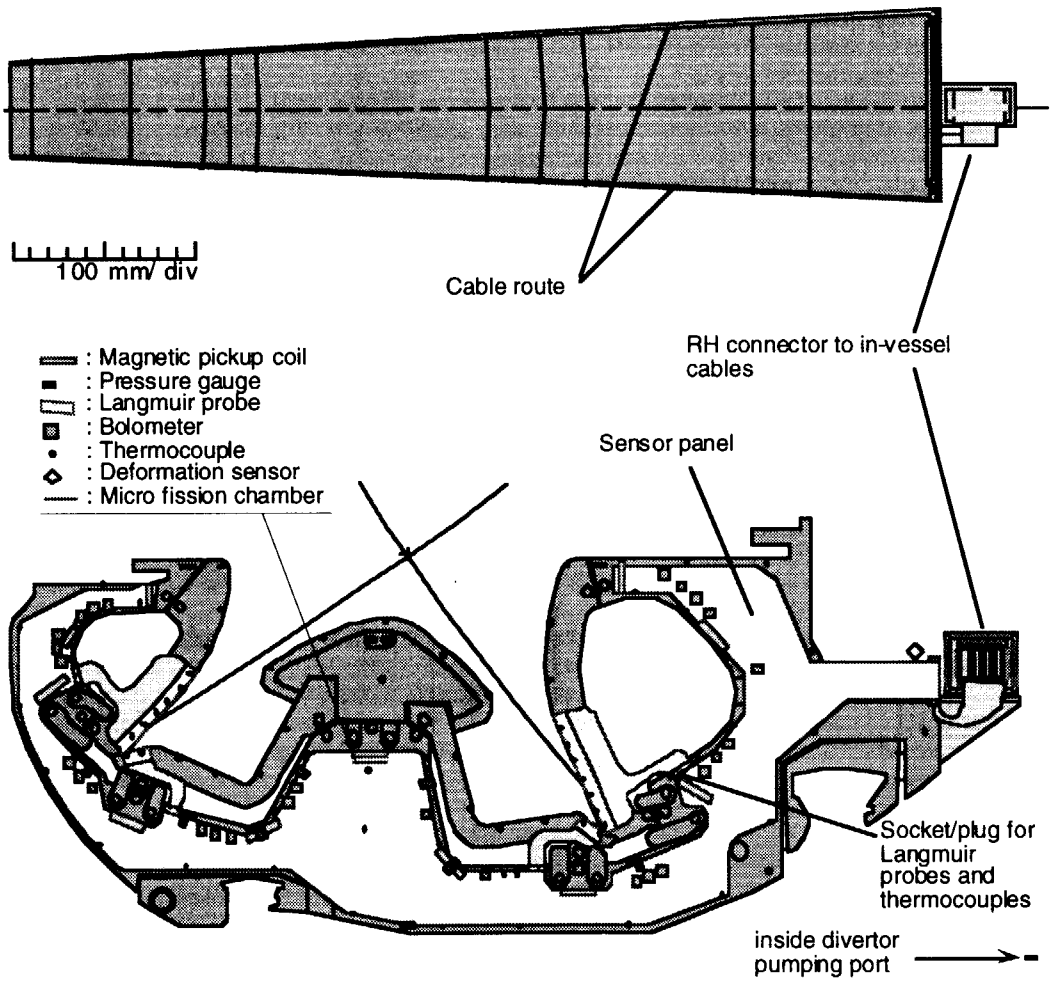

Fig. 3-4 Arrangement of the micro fission chamber in the second divertor cassette. One micro fission chamber is placed under the dome being oriented horizontally.

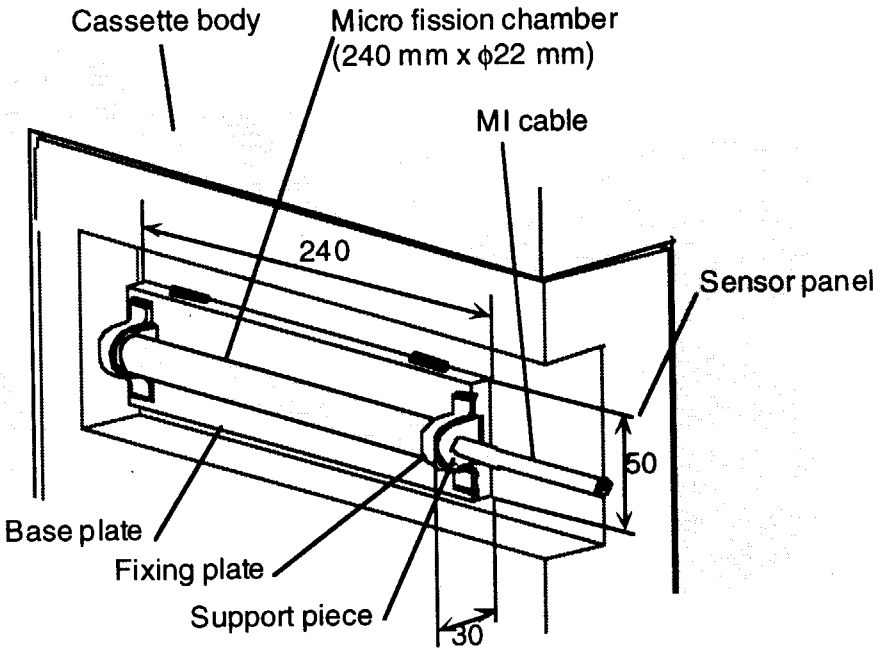

Fig. 3-5 Installation of the micro fission chamber in the second divertor cassette.

3.4 Arrangement of Calibration Detector

As discussed in Section 2.0.9, a high sensitive calibration detector is proposed to be installed between the back plate and vacuum vessel. Now it is considered to mount it on the flame of the diamagnetic loop outside of the back plate as shown in Fig. 2.1-6. We have not evaluated the nuclear heating at the diamagnetic loop position so far. If the heating is severe, we have to change the location such as the back surface of the back plate because it is difficult to cool the detector on the flame of the diamagnetic loop.

The neutron flux monitors has similar high sensitive detectors, it is possible to shear them for the *in-situ* calibration.

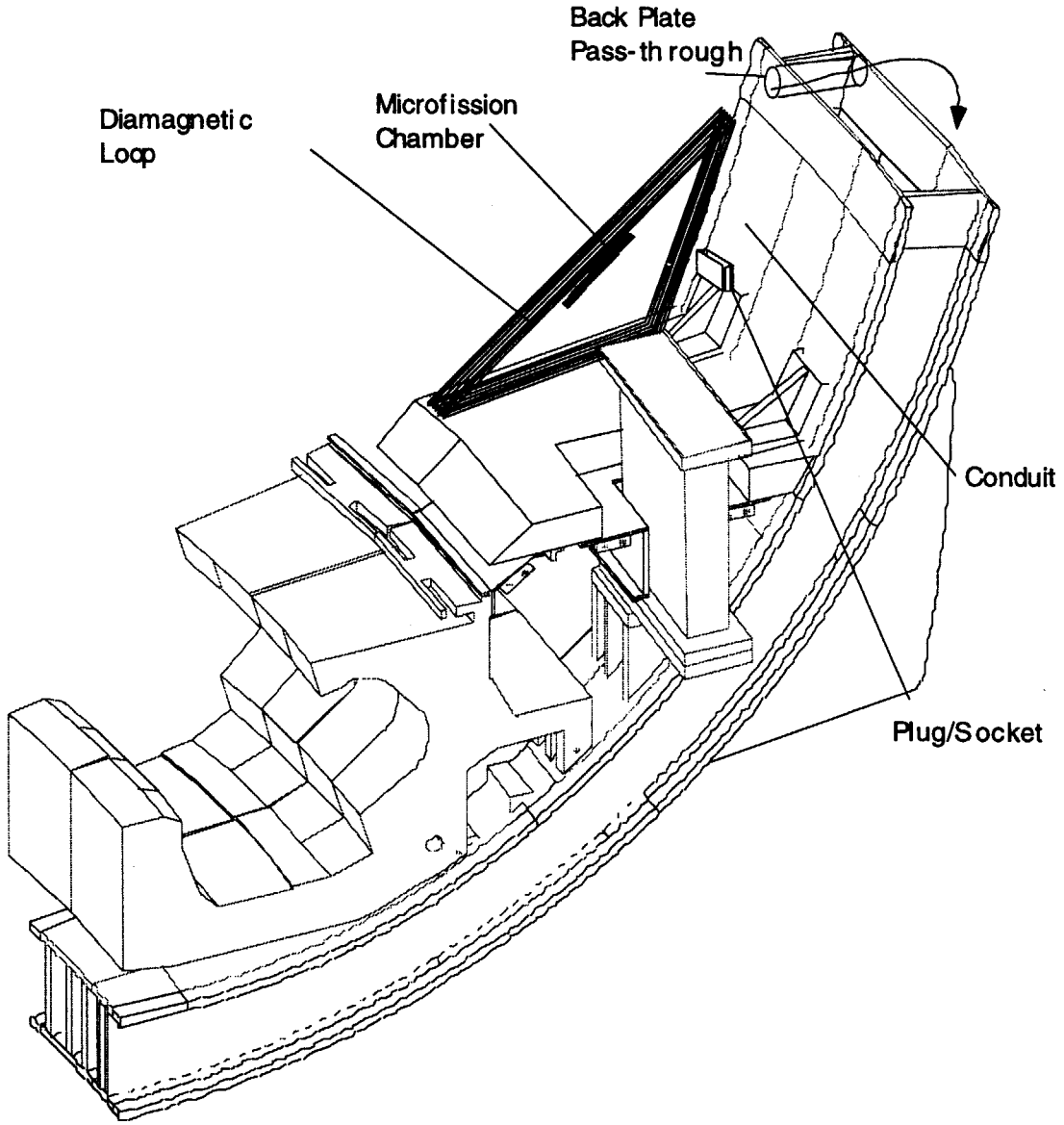

Fig. 3-6. Isometric view of the calibration detector on the flame of the diamagnetic loop.

4. COMPONENT DESIGN DESCRIPTION

4.1 Component List

List of the components is shown in Table 4-1.

Table 4-1. List of Equipment

Component	Quantity	Size (mm)	weight (kg)
^{235}U Micro Fission Chamber	44	$\phi 22 \times 220$	0.6
^{235}U Fission Chamber (Calibration Detector)	2	$\phi 36 \times 410$	1.0
MI Cable	46	$\phi 10$	
Preamplifier	46	$300 \times 190 \times 120$	2
Preamplifier Box	8	$600 \times 600 \times 1200$	120
Integrated Amplifier	24	$480 \times 180 \times 400$	10
BIN Power Supply	8	$300 \times 190 \times 120$	
ADC Module	TBD		
Scalar Module	TBD		
Workstation	1		
Other Digital Modules	TBD		

4.2 Details of Micro Fission Chamber and Calibration Detector

In general, ^{235}U fission chamber is used with moderator of hydrogen rich material such as polyethylene to get the flat response function for all energy range of neutrons for the neutron source strength measurement in fusion experiment. Though the moderation is desirable for micro fission chambers in ITER, we gave it up from following reasons;

- There is no space for the moderator, which needs > 5 cm thickness, between the blanket module and back plate.
- Polyethylene could not used due to high nuclear heating. Even if the moderator would be cooled by water, it could not survive in the loss of coolant accident.

- If the detector is surrounded by the moderator, the detector could not be cooled for the nuclear heating. The moderator plays as thermal insulator.

- In the case of the micro fission chamber, many of incident neutrons are not virgin DT neutron so that moderator is not so important. In other word, we can expect the role of the moderator in the surroundings such as blanket modules and back plate which include much water.

- If the detector is surrounded by the moderator, the detector could not be cooled for the nuclear heating. The moderator plays as thermal insulator.

One of the candidate of the possible moderator is water. If water flows outside of the detector, it can act as both moderator and coolant for the detector. This idea is a future work.

The detail of the micro fission chamber is described in Section 2.1. The sheath is added to the regular micro fission chamber. The electric insulator between the sheath and the housing of the micro fission chamber should have high thermal conductivity to remove the nuclear heat of the detector. One of the candidate is Aluminum Nitride (AlN) which thermal conductivity is 200 W/m•K.

Figure 4-1 shows the schematics of the calibration detector which is the normal size fission chamber with sheath. The chamber contains 0.5 g of ^{235}U, so the sensitivity is 50 times higher than that of the micro fission chamber.

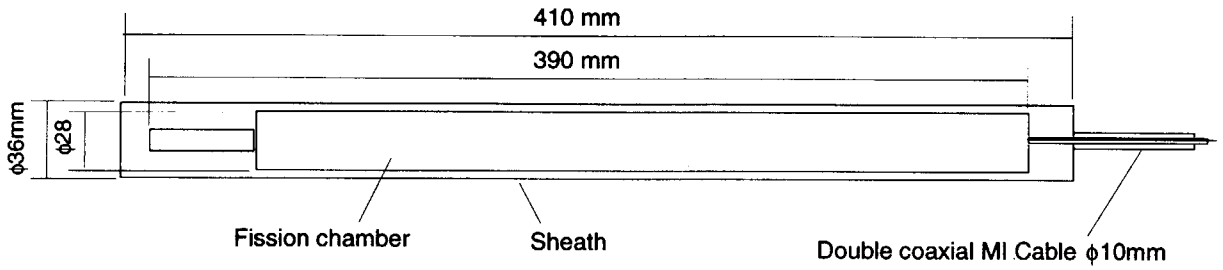

Fig. 4-1. Schematics of the calibration detector which is the normal size fission chamber with sheath.

4.3 Calibration Hardware

In order to satisfy measurement specifications given in Table 1-2, the calibration detectors will require careful absolute calibrations. An essential element of such calibrations is an intense, robust, yet compact DT neutron generator. The generator should

- produce 14 MeV neutrons at an average rate of ~10^{10} n/s,
- have a mean time before maintenance of >1000 hours,
- have a small (<3 mm) effective diameter of the neutron emitting volume (within the larger target diameter),
- be sufficiently compact and portable to allow operation inside the ITER vacuum vessel during initial system calibration and extended maintenance periods, using standard remote handling equipment, for *in situ* mapping of detector responses, and
- be capable of both stand-alone operation and operation controllable by the ITER Command Control and Data Acquisition (CODAC) system.

Of course this calibration hardware can be shared with the neutron flux monitor installed outside the vacuum vessel.

5. SYSTEM PERFORMANCE CHARACTERISTICS

5.1 Operating State Description

5.1.1 Commissioning State

Equipment is installed. ITER has not commenced operation. All electronic equipment is accessible for testing.

5.1.2 Calibration State

Calibration detectors and micro fission chambers are installed and operational. ITER has not commenced operation, and the vacuum vessel is open for in-vessel activities. Neutron generator and transport apparatus are temporarily installed inside ITER vacuum vessel before initial pump-down. Personnel access is excluded in all areas affected by operation of neutron generator.

5.1.3 Experimental Operations State

All equipment is operational. ITER may be in operation. Personnel access is excluded, according to project safety requirements.

5.1.4 Maintenance State

ITER is not in operation. Access to equipment for maintenance activities is determined according to project safety requirements. Basically equipment inside the biological shield are maintenance free.

5.2 Instrumentation and Control

Detectors will require high voltage power supplies, preamplifiers, amplifiers, pulse counting circuitry, Campbelling amplifiers, digital equipment, etc. Preamplifiers should be installed near the detectors. Considering the radiation condition, in the pit near the biological shield is desirable. The integrated amplifier designed for the JT-60U neutron flux monitor which includes a high voltage power supply, pulse amplifier, and Campbelling amplifier is preferable. Exact requirements are TBD.

6. CRITICAL DESIGN AREAS AND R&D ITEMS

6.1 Critical Design Areas

- The response function of the micro fission chambers for the change of the plasma position and neutron source profile should be re-evaluated using more realistic neutronics model in order to justify the number of the detector location.

- Analysis of the electro-magnetic stress in disruption should be done.

- Effect of the temperature on the sensitivity should be evaluated. The technique of the sensitivity calibration should be designed. One of the candidate is that small amount of radio active neutron source such as ^{252}Cf will be mounted near the micro fission chamber. However burn-up of the source should be considered.

- The effect of the change of the gap width between adjacent blanket modules should be evaluated.

6.2 Necessary R&D Items

- The effect of the strong magnetic field on the micro fission chamber should be confirmed experimentally.

of the gap width between adjacent blanket modules should be evaluated.

7. SUMMARY

The absolute neutron source strength measurement is very important for controlling the fusion power in a fusion experimental reactor such as ITER. In present large tokamaks such as JET, TFTR or JT-60U, the neutron source strength measurement has been carried out using ^{235}U or ^{238}U fission chambers installed outside the vacuum vessel. Detection efficiencies of those detectors are easily affected by surrounding equipment such as other diagnostics or heating systems. ITER has a thick blanket and vacuum vessel, so that detectors outside the vacuum vessel can not measure the neutron source strength with sufficient accuracy. We are designing micro fission chambers, which are pencil size gas counters with fissile material inside, to be installed in the vacuum vessel as neutron flux monitors for ITER.

We computed the neutron and gamma flux around the shielding blanket by a two-dimensional neutron calculation, in order to find suitable locations for micro fission chambers. We found that the ^{238}U micro fission chambers are not available because the detection efficiency will increase up to 50% in the ITER life time by breading ^{239}U. We propose that ^{235}U micro fission chambers will be installed on the front side of the back plate in the gap between adjacent blanket modules and behind the blankets at 10 poloidal locations. One chamber will be installed in the divertor cassette just under the dome. We have two toroidal location for the poloidal detectors and four divertor cassette for the divertor detector. Additionally, a couple of the high sensitive detectors are installed for *in-situ* calibration purpose. So the total 44 micro fission chambers and two normal size fission chambers are proposed. Employing both pulse counting mode and Campbelling mode in the electronics, we can accomplish the ITER requirement of 10^7 dynamic range with 1 ms temporal resolution, and eliminate the effect of gamma-rays.

An in-vessel neutron monitor will be affected by changes of the detection efficiency due to the change in the plasma position and neutron source profile. Here we demonstrate by neutron Monte Carlo calculation with three-dimensional modeling that we avoid those detection efficiency changes by installing micro fission chambers at several poloidal locations inside the vacuum vessel. Also the calculation pointed out the DT neutron source with 10^{10} n/s of intensity is needed for the *in-situ* calibration of the micro fission chamber system.

ACKNOWLEDGMENTS

The authors would like to appreciate Dr. S. Sato and Dr. H. Iida for his support on the neutronics calculations. We appreciate Dr. S. Yamamoto for his pioneer work on the micro fission chambers in ITER CDA. This report has been prepared as an account of work assigned to the Japanese Home Team under Task Agreement number S 55 TD 02 FJ within the Agreement among the European Atomic Energy Community, the Government of Japan, the Government of the Russian Federation, and the Government of the United States of America on Cooperation in the Engineering Design Activities for the International Thermonuclear Experimental Reactor ("ITER EDA Agreement") under the auspices of the International Atomic Energy Agency (IAEA).

REFERENCES

[1] O.N. Jarvis, G. Sadler, P. van Bell and T. Elevant, In-vessel calibration of the JET neutron monitors using a ^{252}Cf neutron source: Difficulties experienced, *Rev. Sci. Instrum.* 61: 3172 (1990).

[2] H.W. Hendel, R.W. Palladino, Cris W. Barnes, et al., In situ calibration of TFTR neutron detectors, *Rev. Sci. Instrum.* 61: 1900 (1990).

[3] T. Nishitani, H. Takeuchi, T. Kondoh, et al., Absolute calibration of the JT-60U neutron monitors using a ^{252}Cf neutron source, *Rev. Sci. Instrum.* 63: 5270 (1992).

[4] V.Mukhovatov, H. Hopman, S. Yamamoto, et al., in: *ITER Diagnostics, ITER Documantation Series, No.33*, IAEA, Vienna (1991).

[5] T. Iguchi, J. Kaneko, M. Nakazawa, T. Matoba, T. Nishitani and S. Yamamoto, Conceptional design of neutron diagnostics system for fusion experimental reactor, *Fusion Eng. Design* 28: 689 (1995).

[6] T. Nishitani, K. Ebisawa, T. Iguchi and T. Matoba, Design of ITER neutron yield monitor using microfission chambers, *Fusion Eng. Design* 34-35: 567 (1997).

[7] F.B. Marcus, J.M. Adams, P. Batistoni, et al., A neutron camera for ITER: Conceptual design, in: *Diagnostics for Experimental Thermonuclear Fusion Reactor*, P.E. Stott, G. Gorini and E. Sindoni ed., Plenum Press, New York (1996).

[8] Y. Endo, T. Ito and E. Seki, A counting-Cambelling neutron measurement system and its experimental results by test reactor, *IEEE Trans. Nucl. Sci.* NS-29: 714 (1982).

[9] LANL Group X-6, *MCNP-a general Monte Carlo code for neutron and photon transport version 3A, Report LA-7396-M, Rev.2*, Los Alamos National Laboratory, Los Alamos (1986).

[10] T. Nakagawa, K. Shibata, S. Chiba, et al., Japanese evaluated nuclear data library version 3 revision-2: JENDL-3.2, *J. Nucl. Sci. Technol.* 32: 1259(1995).

[11] T. Nishitani, K. Ebisawa, L.C. Johnson, et al., In-Vessel Neutron Monitor Using Micro Fission Chambers for ITER, in: *Diagnostics for Experimental Thermonuclear Fusion Reactor 2*, P.E. Stott, G. Gorini and E. Sindoni ed., Plenum Press, New York (1998).

国際単位系（SI）と換算表

表1　SI基本単位および補助単位

量	名称	記号
長さ	メートル	m
質量	キログラム	kg
時間	秒	s
電流	アンペア	A
熱力学温度	ケルビン	K
物質量	モル	mol
光度	カンデラ	cd
平面角	ラジアン	rad
立体角	ステラジアン	sr

表2　SIと併用される単位

名称	記号
分，時，日	min, h, d
度，分，秒	°, ′, ″
リットル	l, L
トン	t
電子ボルト	eV
原子質量単位	u

1 eV=1.60218×10^{-19}J

1 u=1.66054×10^{-27}kg

表3　固有の名称をもつSI組立単位

量	名称	記号	他のSI単位による表現
周波数	ヘルツ	Hz	s^{-1}
力	ニュートン	N	m·kg/s^2
圧力，応力	パスカル	Pa	N/m^2
エネルギー,仕事,熱量	ジュール	J	N·m
工率，放射束	ワット	W	J/s
電気量，電荷	クーロン	C	A·s
電位，電圧，起電力	ボルト	V	W/A
静電容量	ファラド	F	C/V
電気抵抗	オーム	Ω	V/A
コンダクタンス	ジーメンス	S	A/V
磁束	ウェーバ	Wb	V·s
磁束密度	テスラ	T	Wb/m^2
インダクタンス	ヘンリー	H	Wb/A
セルシウス温度	セルシウス度	℃	
光束	ルーメン	lm	cd·sr
照度	ルクス	lx	lm/m^2
放射能	ベクレル	Bq	s^{-1}
吸収線量	グレイ	Gy	J/kg
線量等量	シーベルト	Sv	J/kg

表4　SIと共に暫定的に維持される単位

名称	記号
オングストローム	Å
バーン	b
バール	bar
ガル	Gal
キュリー	Ci
レントゲン	R
ラド	rad
レム	rem

1 Å=0.1nm=10^{-10}m

1 b=100fm^2=10^{-28}m^2

1 bar=0.1MPa=10^{5}Pa

1 Gal=1cm/s^2=10^{-2}m/s^2

1 Ci=3.7×10^{10}Bq

1 R=2.58×10^{-4}C/kg

1 rad=1cGy=10^{-2}Gy

1 rem=1cSv=10^{-2}Sv

表5　SI接頭語

倍数	接頭語	記号
10^{18}	エクサ	E
10^{15}	ペタ	P
10^{12}	テラ	T
10^{9}	ギガ	G
10^{6}	メガ	M
10^{3}	キロ	k
10^{2}	ヘクト	h
10^{1}	デカ	da
10^{-1}	デシ	d
10^{-2}	センチ	c
10^{-3}	ミリ	m
10^{-6}	マイクロ	μ
10^{-9}	ナノ	n
10^{-12}	ピコ	p
10^{-15}	フェムト	f
10^{-18}	アト	a

（注）

1．表1－5は「国際単位系」第5版，国際度量衡局1985年刊行による。ただし，1 eVおよび1 uの値はCODATAの1986年推奨値によった。

2．表4には海里，ノット，アール，ヘクタールも含まれているが日常の単位なのでここでは省略した。

3．barは，JISでは流体の圧力を表わす場合に限り表2のカテゴリーに分類されている。

4．EC閣僚理事会指令ではbar，barnおよび「血圧の単位」mmHgを表2のカテゴリーに入れている。

換算表

力	N(=10^{5}dyn)	kgf	lbf
	1	0.101972	0.224809
	9.80665	1	2.20462
	4.44822	0.453592	1

粘度　1 Pa·s(N·s/m^2)=10 P(ポアズ)(g/(cm·s))

動粘度　1m^2/s=10^{4}St(ストークス)(cm^2/s)

圧力	MPa(=10bar)	kgf/cm^2	atm	mmHg(Torr)	lbf/in^2(psi)
	1	10.1972	9.86923	7.50062×10^3	145.038
	0.0980665	1	0.967841	735.559	14.2233
	0.101325	1.03323	1	760	14.6959
	1.33322×10^{-4}	1.35951×10^{-3}	1.31579×10^{-3}	1	1.93368×10^{-2}
	6.89476×10^{-3}	7.03070×10^{-2}	6.80460×10^{-2}	51.7149	1

エネルギー・仕事・熱量	J(=10^7 erg)	kgf·m	kW·h	cal(計量法)	Btu	ft·lbf	eV
	1	0.101972	2.77778×10^{-7}	0.238889	9.47813×10^{-4}	0.737562	6.24150×10^{18}
	9.80665	1	2.72407×10^{-6}	2.34270	9.29487×10^{-3}	7.23301	6.12082×10^{19}
	3.6×10^6	3.67098×10^5	1	8.59999×10^5	3412.13	2.65522×10^6	2.24694×10^{25}
	4.18605	0.426858	1.16279×10^{-6}	1	3.96759×10^{-3}	3.08747	2.61272×10^{19}
	1055.06	107.586	2.93072×10^{-4}	252.042	1	778.172	6.58515×10^{21}
	1.35582	0.138255	3.76616×10^{-7}	0.323890	1.28506×10^{-3}	1	8.46233×10^{18}
	1.60218×10^{-19}	1.63377×10^{-20}	4.45050×10^{-26}	3.82743×10^{-20}	1.51857×10^{-22}	1.18171×10^{-19}	1

1 cal= 4.18605J（計量法）

= 4.184J（熱化学）

= 4.1855J（15℃）

= 4.1868J（国際蒸気表）

仕事率　1 PS(仏馬力)

= 75 kgf·m/s

= 735.499W

放射能	Bq	Ci
	1	2.70270×10^{-11}
	3.7×10^{10}	1

吸収線量	Gy	rad
	1	100
	0.01	1

照射線量	C/kg	R
	1	3876
	2.58×10^{-4}	1

線量当量	Sv	rem
	1	100
	0.01	1

（86年12月26日現在）

DESIGN OF ITER NEUTRON MONITOR USING MICRO FISSION CHAMBERS